Chapter 3

Photosynthetic Reaction Centers: So little time, so much to do

John H. Golbeck
Department of Biochemistry
and
Molecular Biology
The Pennsylvania State University
University Park, PA 16802
USA

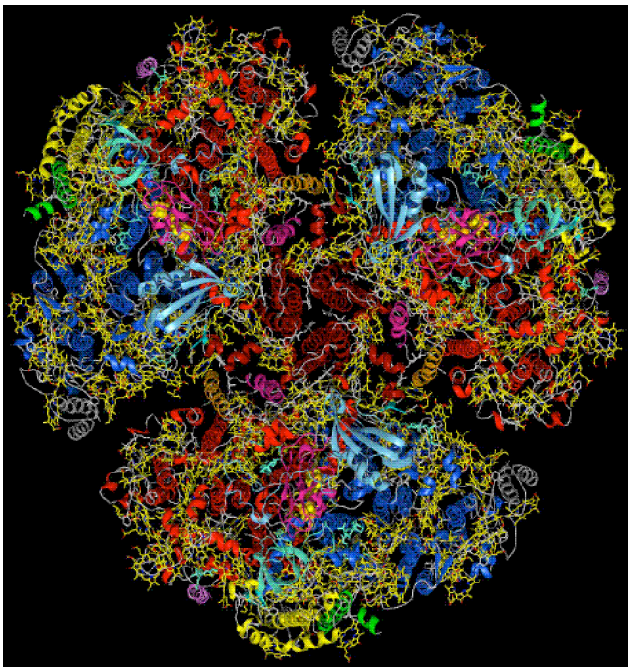

The trimeric Photosystem I reaction center from Synechococcus elongatus *at 2.5 Å resolution. View is from the stromal side looking down into the 3-fold symmetry axis. The chlorophylls are depicted in yellow and the stromal proteins PsaC, PsaD and PsaE are depicted in magenta, light-blue and cyan, respectively, From: P. Jordan, Ph.D. thesis, Freie Universität, Berlin.*

3.1. Introduction

The title and subtitle of this chapter convey a dual meaning. At first reading, the subtitle might seem to indicate that the topic of the structure, function and organization of photosynthetic reaction centers is exceedingly complex and that there is simply insufficient time or space in this brief article to cover the details. While this is certainly the case, the subtitle is additionally meant to convey the idea that there is precious little time after the absorption of a photon to accomplish the task of preserving the energy in the form of stable charge separation.

The difficulty is there exists a fundamental physical limitation in the amount of time available so that a photochemically induced excited state can be utilized before the energy is invariably wasted. Indeed, the entire design philosophy of biological reaction centers is centered on overcoming this physical, rather than chemical or biological, limitation.

In this chapter, I will outline the problem of conserving the free energy of light-induced charge separation by focusing on the following topics:

3.2. Definition of the problem: the need to stabilize a charge-separated state.
3.3. The bacterial reaction center: how the cofactors and proteins cope with this problem in a model system.
3.4. Review of Marcus theory: what governs the rate of electron transfer in proteins?
3.5. Photosystem II: a variation on a theme of the bacterial reaction center.
3.6. Photosystem I: structure, function and organization of the cofactors and proteins.
3.7. Unifying themes in photosynthesis: a common photochemical motif in all of nature.

3.2. Definition of the Problem: The Need to Stabilize a Charge-Separated State.

In this section, I will outline the problems associated with extracting free energy from a photochemically generated charge-separated state.

3.2.1. Definition of the Problem: The Absorption of Light

The absorption of light by a chromophore occurs in ca. 10^{-15} sec from the ground electronic state of a molecule (Figure 1). If, for the purpose of this discussion, we suppose that the second singlet excited state is populated, internal conversion will result in the loss of vibrational and rotational energy and the transfer of electronic energy to the first excited singlet state in ca. 10^{-12} sec. The residence time in the ground vibrational and rotational level of the first excited state is, in comparison, relatively long, up to 10^{-8} sec, for chlorophylls.

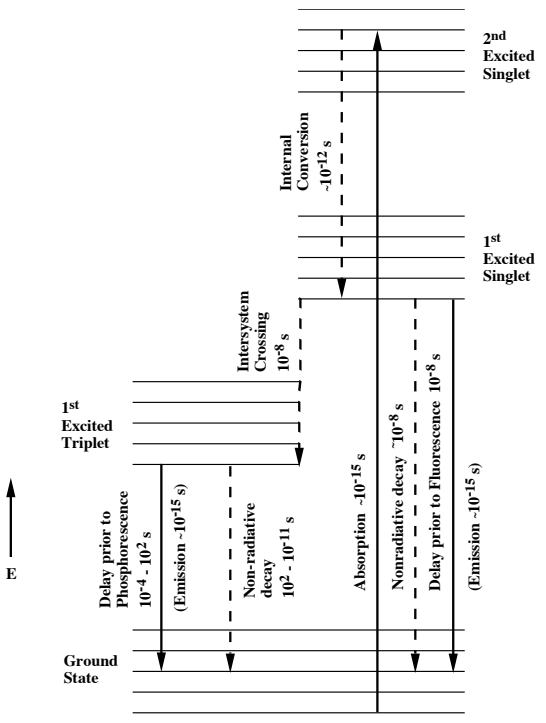

Figure 1. Lifetimes of absorption, fluorescence and phosphorescence at the equilibrium internuclear distance of the ground state. The energy levels are not depicted to scale.

At this point, three processes compete for de-excitation: non-radiative decay (thermal processes), intersystem crossing (formation of triplet states), and fluorescence (re-emission of a photon). In any given molecule, the process with the shortest lifetime will prevail. Hence, in the absence of a competing process, fluorescence represents the upper limit of an excited state lifetime. A corollary to this statement is that every molecule that absorbs light would fluoresce were it not for the existence of faster de-excitation processes.

Take home lesson #1: In photosynthesis, the energy of the photon can be productively utilized only between the limits of absorption (10^{-15} sec) and fluorescence (10^{-8} sec) of the chlorophyll molecule.

There exists a fourth possible fate for the singlet excited state: photochemistry, which is electron transfer to a separate molecule, producing a charge-separated (cation-anion) pair. For this to happen, the excited state must be followed by a rapid electron transfer step, one that exceeds the rates of any de-excitation process.

For a quantum yield ≥ 0.99 (*definition:* the ratio of the number of charge separated states divided by the number of photons used), this step must be several orders-of-magnitude faster than 10^{-8} sec if fluorescence is the primary de-excitation mode. Thus, charge separation must occur within ca. 10^{-10} sec (100 ps) following the absorption of the photon. Clearly, any design of a photochemical reaction center that depends on simple diffusion chemistry between two molecules in solution will not succeed.

Chlorophyll *a* is the major light absorbing and the sensitizing (S) chromophore in oxygenic photosynthetic systems, including Photosystem I and Photosystem II in cyanobacteria, algae and higher plants (Figure 2). In this role it has several major advantages; it absorbs light in the red and blue regions of the visible spectrum, it has a large molar extinction coefficient, and it has a high fluorescence yield.

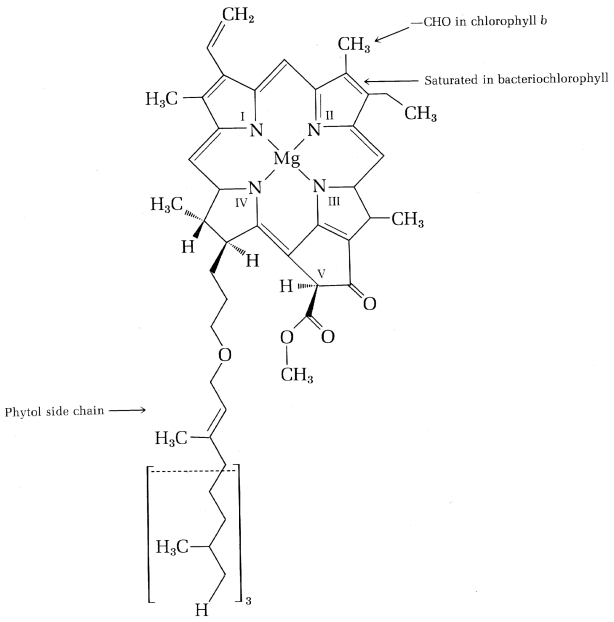

Figure 2. Structure of chlorophyll a, the antenna and sensitizer molecule of Photosystem I. Note that pheophytin a lacks the central Mg^{2+} atom; chlorophyll b has a –CHO group in place of the CH_3 group in ring II; bacteriochlorophyll, a has a single bond in place of the double bond in ring II; bacteriopheophytin, a has a single bond in place of the double bond in ring II and lacks the central Mg^{2+} atom; and bacteriochlorophyll b has a –CHO group in place of the methyl group and a single bond in place of the double bond in ring II.

Why should this matter? It does because the absorption of a photon by a molecule of chlorophyll *a* leads within 10^{-12} sec to the lowest vibrational and rotational level of the first excited singlet state. The absence of non-radiative decay routes lengthens the excited state lifetime to the maximum allowed for the extraction of energy.

This excited state is stable for up to 10^{-8} sec, after which the molecule returns to the ground state with the emission of a photon. This is the maximum interval allowed for the extraction of work via photochemistry. In contrast, a non-fluorescent molecule would have a much shorter lifetime in the singlet excited state, making it even more difficult to extract the energy of the excited state in the time available.

Take home lesson #2: Chlorophyll a is an extremely good chromophore for photosynthetic systems because it is both an efficient absorber of light and because the excited state lifetime is long.

Problem 1. If the energy in a photon, E = $h\nu$ = hc/λ where h is Planck's constant, and ν, λ and c are the frequency, wavelength, and speed of light, what is the energy, in Joules and electron-volts (eV), of the photon absorbed by (i) the bacterial photosynthetic reaction center special pair at its peak at 865 nm in the near-infrared region, and (ii) the Photosystem II reaction center at 680 nm in the visible region, and (iii) the Photosystem I reaction center at 700 nm at the edge of the visible region?

3.2.2. Definition of the Problem: Creation of Charge Separation

In principle, an immobilized pair of donor-acceptor molecules could be used for rapid electron transfer. In the following example, we will assume that the sensitizer also serves the role of electron donor:

$$\mathbf{S-A} + h\nu \rightarrow \mathbf{S^*-A} \rightarrow \mathbf{S^+-A^-}$$

The electron in the excited singlet state of the sensitizer **S** finds an electron deficient molecule within van der Waals distance, and electron transfer results, creating a reductant $\mathbf{A}^-$. Meanwhile, the hole left in the sensitizer results in the creation of an oxidant, $\mathbf{S}^+$. Thus, a charge-separated state $\mathbf{S}^+ \mathbf{-} \mathbf{A}^-$ is produced.

$\mathbf{S}^+$ meanwhile could become reduced by a reductant in solution, $\mathbf{A}^-$ could become oxidized by an oxidant in solution, and the chemical free energy of the photon could thereby be extracted to carry out useful work. The problem with this scheme is that $\mathbf{S}^+$ and $\mathbf{A}^-$ are in very close proximity, making $\mathbf{A}^-$ the closest reductant to $\mathbf{S}^+$ and the $\mathbf{S}^+$ the closest oxidant to $\mathbf{A}^-$. Hence, the

charge-separated state would be short-lived.

In practice, the charge-separated state has a several possible fates, including:

$$S^+ - A^- \rightarrow (S^* - A) \rightarrow S - A + h\nu$$

or

$$S^+ - A^- \rightarrow (S^* - A) \rightarrow S - A + \Delta$$

where $h\nu$ is a fluorescent photon and **Δ** is heat released as vibrational and rotational energy.

In biological reaction centers, the first charge-separated state between the chlorophyll donor and the chlorophyll acceptor has a lifetime of ca. 10 ns. Because diffusion chemistry is so much slower, a simple donor-acceptor pair is not very useful in a biochemical environment.

3.2.3. Definition of the Problem: Stabilization of Charge Separation

What can be done to solve the problem of the short lifetime of the charge-separated state? One solution is to extend the distance between S^+ and A^- by adding a second closely spaced acceptor molecule, A_2:

$$S - A_1 - A_2 + h\nu \rightarrow S^* - A_1 - A_2 \rightarrow S^+ - A_1^- - A_2 \rightarrow S^+ - A_1 - A_2^-$$

What incentive would the electron have to move from A_1^- to A_2? This could happen by introducing a drop in Gibbs free energy between A_1 and A_2, thereby altering the equilibrium constant. While this results in a loss of thermodynamic efficiency (*i.e.* the free energy conserved as $D^+ A^-$ divided by the energy of the photon), this is the price that must be paid for an increased lifetime of the charged-separated state. A similar strategy might be to add a second closely spaced donor molecule, **D**:

$$D - S - A_1 + h\nu \rightarrow D - S^* - A_1 \rightarrow D - S^+ - A_1^- \rightarrow D^+ - S - A_1^-$$

In this example, the hole would be transferred from S^+ to **D** (which is equivalent to an electron transfer from **D** to S^+) if the equilibrium constant were similarly altered by introducing a drop in Gibbs free energy between **D** and S^+.

Take home lesson #3: an increased lifetime of the charge-separated state can be purchased by a loss of Gibbs free energy in a system that contains additional electron acceptors or donors.

In summary, the working strategy of a photosynthetic reaction center involves:

- Efficient absorption by a chromophore/sensitizer,
- Rapid and efficient charge separation between the sensitizer and an acceptor,
- Rapid charge delocalization with an second donor or acceptor to increase the lifetime of the charge-separated state.

Therefore, the key to understanding the efficiency of photosynthetic electron transfer is the relationship between the rate of electron transfer and the parameters of distance, Gibbs free energy, and reorganization energy.

3.3. The bacterial reaction center: how the cofactors and proteins cope with this problem in a model system.

However, before we begin to examine this relationship in depth, we need to look at how a naturally occurring photosystem is constructed and how it operates. We shall use the bacterial reaction center (*Rhodobacter sphaeroides*) for this purpose because it is the simplest and best-understood model system.

3.3.1. Global View of the Bacterial Reaction Center: Overall Function

If charge separation is the goal of photochemical reaction centers, just what are the products of this reaction?

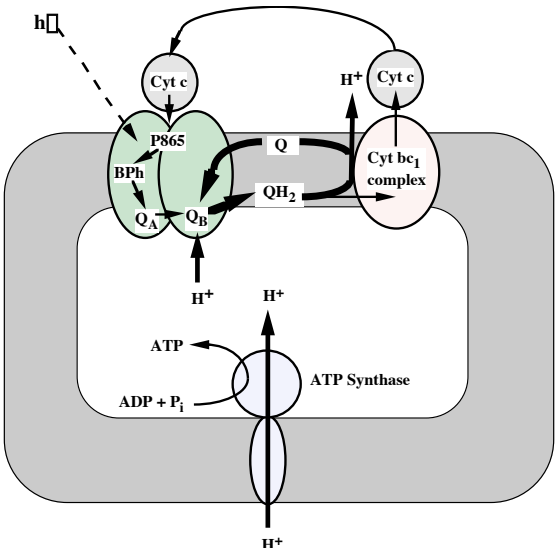

Figure 3 Overall operation of the bacterial reaction center. The design philosophy is to promote a series of embedded cycles, one involving electrons and another involving protons. The reaction center reduces quinone to quinol, and the cytochrome bc_1 complex oxidizes quinol to quinone. During this process, four protons are translocated across the membrane, producing an electrochemical gradient. The gradient represents the stored energy of the photon, which is used by ATP synthase to produce the final product of bacterial photosynthesis, ATP.

The short answer is that the bacterial reaction center reduces ubiquinone to dihydroubiquinol in a reaction that consumes two protons on the inside of a closed biological membrane (Figure 3). The dihydroubiquinol is oxidized by the cytochrome bc_1 complex (in a mechanistically complex reaction termed the protonmotive Q-cycle) in a reaction that translocates up to four protons to the outside of the membrane. The resulting electrochemical proton gradient ($\Delta\square_{H+}$) represents stored free energy derived from the photon. [See Chapter 1 in this textbook, section 1-8,4]. The energy in the electrochemical proton gradient is converted to chemical bond energy in the synthesis of adenosine triphosphate (ATP) by the membrane-bound ATP-synthase enzyme.

3.3.2. Global View of the Bacterial Reaction Center: Internal Operation

The bacterial reaction center uses a strategy of transferring the electron from the primary electron acceptor, bacteriopheophytin *a*, to two additional electron acceptor molecules, termed Q_A and Q_B, to stabilize charge separation in a suitable time domain. Both are quinones (Figure 4).

A soluble reduced cytochrome c^{2+} reduces the oxidized bacteriochlorophyll sensitizer with a peak absorbance at 865 nm, termed P_{865}, thereby preventing the charge recombination between oxidized P_{865}^{+} and the electron Q_B^{-}. The net effect is that reduced Q_B^{-} has no oxidized donor in close proximity, thus allowing for a long-lived product P_{865} Q_A Q_B^{-}. The oxidized cytochrome c^{3+} molecule diffuses from the membrane-bound reaction center and accepts an electron from the cytochrome bc_1 complex.

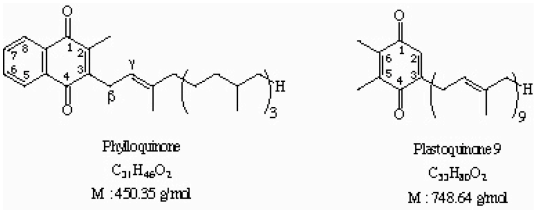

Figure 4 Structures of oxidized phylloquinone, the intermediate electron acceptor in Photosystem I, and oxidized plastoquinone, the intermediate electron acceptor in Photosystem II. Note the naphthoquinone and benzoquinone head groups and the extended phytyl-like tail.

3.3.3. Global View of the Reaction Center: Operation of the Cycle

The first photon absorbed leads to the charge-separated state (Figure 5):

$$P_{865}\ \mathbf{Q_A}\ \mathbf{Q_B^-}$$

The second photon absorbed leads to the unstable charge-separated state:

$$P_{865}\ \mathbf{Q_A^-}\ \mathbf{Q_B^-}$$

One proton is taken from the medium as the electron moves from Q_A to Q_B, resulting in:

$$P_{865}\ \mathbf{Q_A}\ \mathbf{(Q_BH)^-}$$

A second proton is subsequently taken up from the medium, resulting in:

$$P_{865}\ \mathbf{Q_A}\ \mathbf{(Q_BH_2)}$$

The doubly reduced and protonated ubiquinol QH_2 has a low affinity for the Q_B binding site and diffuses in the membrane *to* the cytochrome bc_1 complex. The Q_B binding site has a high affinity for oxidized ubiquinone, which diffuses in the membrane *from* the cytochrome bc_1 complex.

The net result is that the Q_B site is 'recharged' with fresh quinone, thereby allowing another round of light-induced reduction of ubiquinone to ubiquinol.

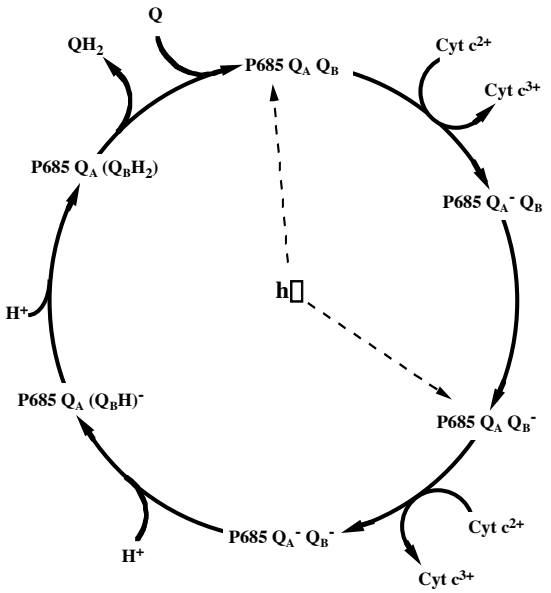

Figure 5. Cyclic operation of the bacterial reaction center. Note that Q_A is only capable of a single electron reduction to the semiquinone radical state, whereas Q_B is capable of double reduction followed by double protonation to the fully-reduced hydroquinone state. The reduced hydroquinone is loosely bound to its site and is displaced by an oxidized quinone for another round of light-induced turnover.

3.3.4. Global View of the Bacterial Reaction Center: Cofactor Arrangement

The atomic resolution x-ray crystal structure of the purple bacterial reaction center from *Rhodobacter sphaeroides* (PDB entry 1AIJ) shows that the L and M subunits form a heterodimeric core of membrane-spanning □-helices arranged along a pseudo-C_2 symmetry axis (Figure 6). The most striking feature of the structure is that that there are no charged amino acids within the membrane-spanning □-helices. The electron transfer components are embedded entirely within the hydrophobic core.

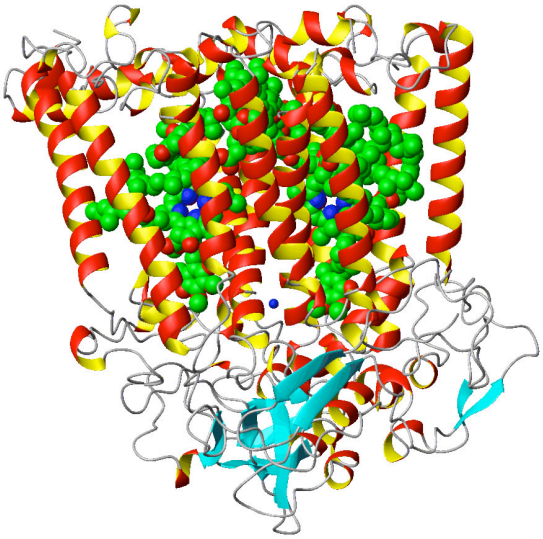

Figure 6 Depiction of the Rhodobacter sphaeroides reaction center. The □-helices are depicted in red/yellow; □-sheets in cyan; the bacteriochlorophyll a and bacteriopheophytin a molecules in green; and the non-heme iron in blue. The menbrane thickness can be estimated by the length of the membrane-spanning □-helices. From the Jena Image Library for Biological Molecules; http://www.imb-jena.de/IMAGE.html

As shown in Figure 7, two molecules of bacteriochlorophyll *a* function in a dimer configuration as the primary electron donor. A bridging bacteriochlorophyll *a* molecule serves as a transient intermediate electron acceptor, which is difficult to observe spectroscopically because of the short lifetime, and a bacteriopheophytin *a* serves as the primary electron acceptor. A

tightly bound ubiquinone, Q_A, is the secondary electron acceptor, and a mobile ubiquinone, Q_B, is the terminal electron acceptor.

Spectroscopic and structural studies show:

- The electron transfer cofactors are very closely spaced.
- Only one branch of cofactors functions in electron transfer from P_{865} to Q_B.
- The non-heme iron can be replaced with Zn^{2+} without loss of function.

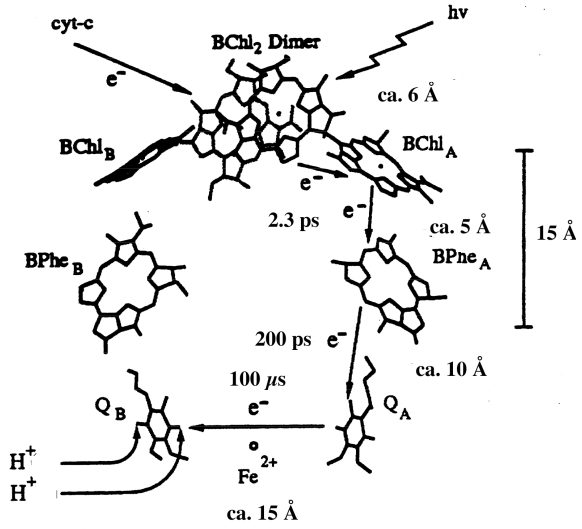

Figure 7. Cofactors of the bacterial reaction center. The edge-to-edge distances between the cofactors are depicted along with the electron transfer rates. The distances are only approximate and refer to the closest approach of the aromatic rings (sufficiently accurate for the purpose of this discussion). Note the pseudo C_2 axis of symmetry that spans the bacteriochlorophyll a dimer and the non-heme iron.

As shown in Figure 7, the approximate edge-to-edge distance between the bacteriochlorophyll *a* dimer, P_{865}, and the bridging bacteriochlorophyll *a* molecule is ca. 6 Å, and the distance between the bridging bacteriochlorophyll *a* and the bacteriopheophytin *a* acceptor is ca. 5 Å. The electron is transferred between P_{865}* and the bacteriopheophytin *a* acceptor, a distance of ca. 10 Å, in 2.8 ps. The bacteriopheophytin *a* acceptor is separated from Q_A by ca. 10 Å, and the electron is transferred in 200 ps. Finally, the electron is transferred from Q_A^- to Q_B in 100 μs over a distance of 15 Å.

Clearly, there is a relationship between distance and rate of electron transfer. One can raise the following two questions: what factors govern the rate of each electron transfer step, and what is the role of the protein?

Problem 2. The fastest chemical reaction known in biology is the first electron transfer in bacterial photosynthesis, in which an initial distance of ca. 6 Å is covered in a time period of 2.8 ps. The next fastest biological reaction is the electron transfer step from reduced BPh^- to Q_A, in which a distance of ca. 10 Å is covered in a time period of 200 ps. Calculate the average speed of these electron transfer steps in km/h. How fast is this relative to the speed of light (10^8 m sec^{-1}), the cruise speed of a Boeing 747 (1000 km h^{-1}) or a fast walk (6 km h^{-1})?

Why does speed matter in photosynthetic systems? The answer has to do with our previous finding that the initial electron transfer process must occur faster than the fluorescence lifetime of the singlet excited state of the chlorophyll sensitizer molecule. In practice, this means that the electron transfer cofactors must be exceedingly close together in photosynthetic systems

3.4. Review of Marcus Theory: What Governs the Rate of Electron Transfer in Proteins?

We will now briefly review the relationship between rate, distance, and driving force in biological electron transfer reactions.

3.4.1. Review of Marcus Theory: Overview of Proteins

With metal ions in solution, electron transfer occurs when the two are in van der Waals contact, but with metal cofactors in proteins, electron transfer must occur over distances up to 15 Å or greater. Rates of chemical reactions are described along a potential energy surface in traditional transition state theory. As reactants gain energy from thermal collisions, they overcome an activation energy barrier to achieve the transition state, after which they spontaneously decay to product.

In traditional theory, the formation of the transition state invariably leads to product. This is a so-called 'adiabatic' reaction. In thermodynamics, this term is used to indicate that no heat flows into or out of a system, but in electron transfer theory, it means that the system makes no transition to other states, remaining on the lower-order electronic surface.

In traditional theory, electron transfer occurs at the intersection of the two potential energy surfaces, a condition attained by thermal fluctuations of the two nuclei. The horizontal displacement represents the adjustment of the nuclear coordinates to the different electronic configurations for the reactant ($\mathbf{D^- A}$) and product ($\mathbf{D A^-}$).

In proteins, due to the fact that the electron transfer must occur between metals cofactors that are separated by large distances, an additional electronic term is required for electron transfer, the 'electronic matrix coupling element'. This term effectively removes the degeneracy of the reactant and product states at the intersection.

3.4.2. Review of Marcus Theory: Fermi's Golden Rule

Fermi's Golden Rule applies to long-range electron transfer processes in proteins, in which the electron donors and acceptors are only weakly coupled due to their long-distance separation. These are so-called 'non-adiabatic reactions':

$$k_{et} \mu 2\pi/h * |H_{AB}|^2 * (FC) \qquad (1)$$

where k_{et} is the electron transfer rate. h is Planck's constant $|H_{AB}|$ is the electronic matrix coupling element, and FC is the Franck-Condon factor.

The rule has two terms. The first term, $|H_{AB}|^2$, states that the electron transfer rate is proportional to the square of the weak coupling of the reactant and product electronic states. The donor and acceptor wave functions must span the space separating the donor and acceptor molecules; hence, this parameter concerns the variable of distance. The overlap of wavefunctions falls off exponentially with edge-to-edge distance between cofactors, modified by a term that is different for free space, proteins, and covalently bound molecules. We will examine this factor more closely later.

The second term, the Franck Condon factor, relates to the nuclear position of the reactant molecules and their environment, and is similar to traditional transition state theory. This term relates to the overlap of the reactant and product harmonic oscillators, and includes such factors as the effect of temperature, the reorganization energy, and the Gibbs free energy difference between the products and reactants. We shall examine this term first.

3.4.3. Review of Marcus Theory: The Franck-Condon Term

Marcus used harmonic oscillators as descriptions of electron donors and acceptors. However, instead of using two separate potential energy surfaces for the reactants, he used a single surface to describe the potential energy of the precursor complex as a function of its nuclear configuration (Figure 8).

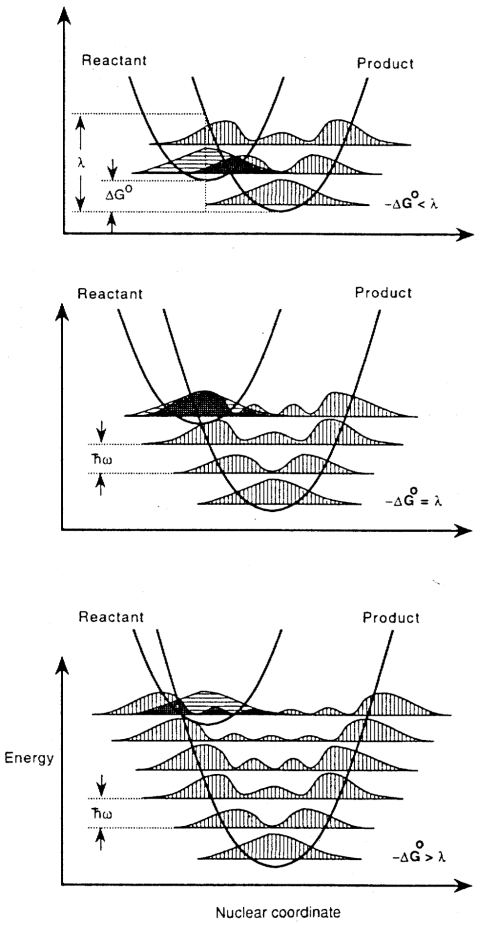

Figure 8. Intersecting parabolic potential energy surfaces used to represent classical reactant and product harmonic oscillators for three electron transfer reactions with different free energies. Note that in the top panel, $-\Delta G^0 < \lambda$, in the middle panel $-\Delta G^0 = \lambda$ and in the lower panel $-\Delta G^0 > \lambda$. The quantum mechanical harmonic oscillator wavefunctions are superimposed on these parabolas; the fastest electron transfer occurs at maximum overlap. The optimum rate of electron transfer therefore occurs when $-\Delta G^0 = \lambda$. Reproduced with permission from Moser et al. 1992; http://www.nature.com/

The latter includes its rotational, vibrational, and translational motion including those of the molecules in the surrounding solution. In keeping with this idea, a single surface was used for the product complex. Marcus recognized that the free energy of activation, $\Delta G^{\ddagger}$, has a quadratic dependence on the reorganization energy (λ) and on the standard Gibbs free energy difference between the products and reactants (ΔG^0) according to the expression $\Delta G^{\ddagger} \mu [-(\Delta G^0 + \lambda)^2/4\lambda]$. The rate of electron transfer, k_{et}, is related to these terms according to the following equation:

$$k_{et} \mu exp [-(\Delta G^0 + \lambda)^2/4\lambda k_B T] \qquad (2)$$

where k_B is Boltzmann's constant, and T is the absolute temperature. [For derivation of the Franck-Condon term, see Chapter I, section I-13 in this textbook].

The expression for $\Delta G^{\ddagger}$ defines a parabola. As $-\Delta G^0$ increases, the rate of electron transfer increases, but only until $-\Delta G^0 = \lambda$, at which point the rate is maximum. As $-\Delta G^0$ increases further, the rate of electron transfer decreases. There are hence three regions to the parabola. In the 'normal' region, $-\Delta G^0 < \lambda$, and k_{et} increases if $-\Delta G^0$ increases or if l decreases. At the optimum, $-\Delta G^0 = \lambda$, k_{et} is maximum. In the 'inverted' region, $-\Delta G^0 > \lambda$, and k_{et} decreases if $-\Delta G^0$ increases or if λ decreases.

In Figure 9, the rate of electron transfer is shown as a function of ΔG^0 for two photosynthetic reactions; the physiologically-useful electron transfer over ca. 10 Å from BPh^- to Q_A (top), and the physiologically-unproductive backreaction over 22 Å from Q_A^- to P^+.

An analysis over a range of temperatures suggests a constant value of l of 0.7 eV in proteins, and a common hλ of 70 meV (basically, the width of the parabola), which is over twice the 25 meV Boltzmann energy (kT) available at room temperature. Although I will not discuss this parameter further, the high frequency protein vibrational modes are important because they are likely to be coupled to electron transfer.

The most striking feature of this plot is the *relative* insensitivity of the electron transfer rate to the thermodynamic driving force, especially at values near the optimum rate.

Take home lesson #4: Nature does not appear to rely primarily on altering the Gibbs free energy between product and reactant to modulate the rate of electron transfer in proteins.

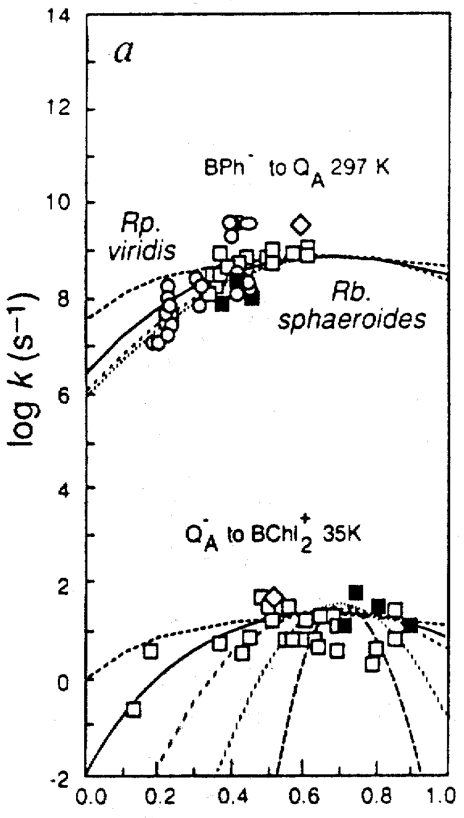

Figure 9. *Free energy dependence on electron transfer rate in the bacterial reaction center. The Gibbs free energy was changed by replacing the native Q_A with compounds with different redox potentials. The fits are with □ = 0.7 eV and with hw = 150 meV (dotted), 70 meV (solid, 30 meV (large, dashed) and 10 meV (small, dashed). Reproduced with permission from Moser et al., 1992;* http://www.nature.com/

Problem 3. Calculate the drop in Gibbs free energy that would be needed to accelerate the electron transfer rate between two cofactors by a factor of 10, given □ = 0.7 eV in proteins and no change in distance or reorganization energy.

3.4.4. Review of Marcus Theory: The Electronic Coupling Term

The electronic coupling term depends on the distance between the electron donor and electron acceptor, and the nature of the intervening medium. The equation for the electronic coupling term is:

$$| H_{AB} |^2 \mu \; exp(-\beta R) \qquad (3)$$

where H_{AB} is the coupling probability at close contact, R is the edge-to-edge distance between the electron donor and the electron acceptor, and □ depends on the nature of the intervening medium (Figure 10). □ is 0.7 $Å^{-1}$ in covalently bonded molecules, 1.4 $Å^{-1}$ in proteins and 2.8 $Å^{-1}$ in a vacuum.

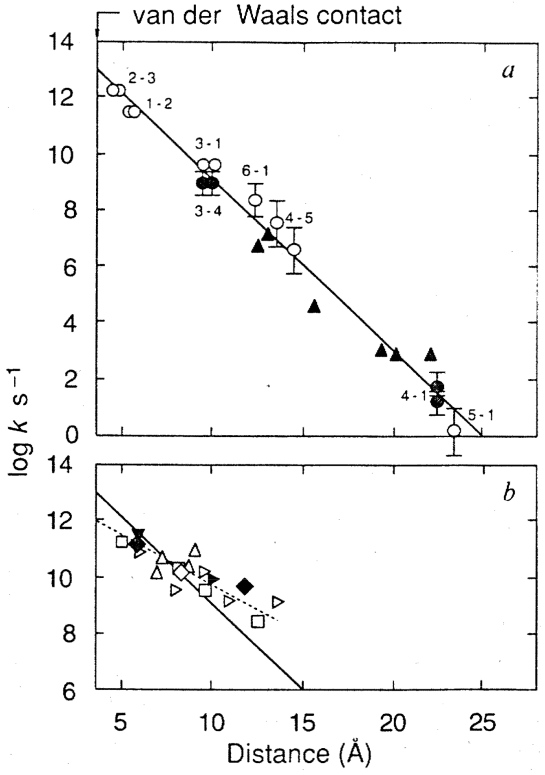

Figure 10. Free energy optimized rate vs edge-to-edge distance relationships for electron transfer in (top) the photosynthetic system and (bottom) in the Ru-cyt c and Ru-Mb system. The vertical line represents van der Waals contact. Reproduced with permission from Moser et al., 1992; http://www.nature.com/

In proteins, this corresponds to a 10-fold change in the rate of electron transfer for every 1.7 Å of distance. Therefore, unlike the weak contribution by the Franck-Condon term, the rate of electron transfer in proteins is strongly sensitive to the electronic coupling term.

Take home lesson #5: Biological systems take good advantage of altering the distance between product and reactant to modulate the rate of electron transfer in proteins.

3.4.5. Review of Marcus Theory: The Moser-Dutton Simplification

Given the finding of a constant h□ = 70 meV and □ = 0.7 eV in proteins, Moser and Dutton (Moser et al. 1992) simplified the equation to:

$$k_{et} = 10 \text{ ^ } [15 - 0.6R - 3.1(\Delta G^0 + \square)^2 / \square] \quad (4)$$

or

$$\log_{10} k_{et} = 15 - 0.6R - 3.1(\Delta G^0 + \square)^2 / \square \quad (5)$$

This simplified equation states that when electron transfer cofactors are at van der Waals distance, electron transfer rates are 10^{15} sec^{-1}.

There are three correction terms. One involves distance: as the spacing between electron transfer cofactors increases, the logarithm of the rate decreases by 0.6*R, where R is the edge-to-edge distance. The second involves the difference in the standard Gibbs free energy between reactants and products, and the final term involves the reorganization energy, □. Note that when $-\Delta G^0 = \square$, the rate is optimum; any increase *or* decrease in Gibbs free energy relative to the reorganization energy leads to a lower (suboptimal) rate of electron transfer.

Thus, one can calculate the optimum rate of electron transfer (to within an order-of-magnitude) by simply knowing the edge-to-edge distance between donor and acceptor pairs (Figure 11).

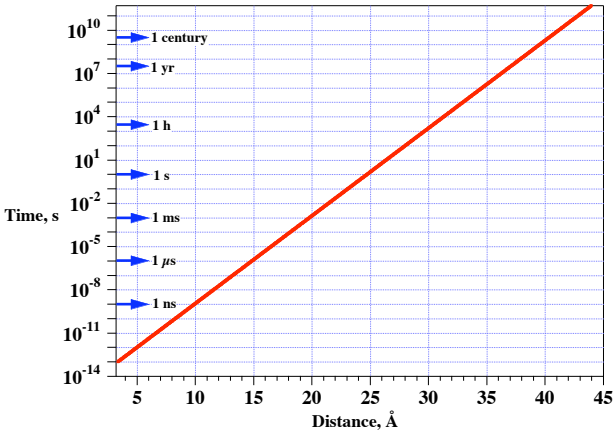

Figure 11. The Moser-Dutton simplification of the Marcus relationship: electron transfer rate in proteins as a function of distance, assuming optimal conditions, i.e. $-\Delta G^0 = \square$.

Note that when the edge-to-edge distance between cofactors is 10 Å, the electron transfer rate is ca. 1 ns. Doubling this distance to 20 Å results in an electron transfer rate of ca. 1 ms, and a distance of 30 Å results in a rate of almost an hour.

This relationship may explain, in part, why an energy-transducing biological membrane is >30 Å in thickness: charge recombination between an oxidized cofactor on one side and a reduced cofactor on the other side of the membrane must be prevented on timescales that these cofactors carry out their respective biochemical roles in metabolism.

To summarize:

- □ is usually considered constant in proteins, although a more sophisticated treatment is available that takes into account variations of □ in proteins (see below).

- ΔG^0 can modulate the rate up to 10^5 fold over the available range of 0 to 1.3 eV in biochemical systems. In reality, however, ΔG^0 is usually constrained by the need to conserve free energy,

- □ is difficult to measure experimentally but is typically assumed to be 0.7 eV in a protein mileu.

- R, however, is a free variable that is effective over a 10^{12} fold range with few restrictions.

A more complete treatment has been developed (Page et al., 1999) that takes into account variations in polypeptide structure. This equation includes a packing density (□) of protein atoms in the volume between redox centers to account for variations in □:

$$Log_{10}k_{et}=13-(1.2-0.8\square)(R-3.6)-3.1(\Delta G^{0}+\square)^{2}/\square$$

where □ is the fraction of the volume between redox cofactors that is within the united van der Waals radius of intervening atoms.

Thus, although the fundamental concepts of electron transfer have been refined and expanded in recent years, equation (4) will be sufficient to make important points regarding the placement of cofactors in biological systems.

Take home lesson #6: In bioenergetic complexes, metal centers and organic cofactors exist in part to cope with the problem of long-distance electron transfer across membranes.

3.4.6. Review of Marcus Theory: Implications for Photosynthetic Systems

If a 40 Å biological membrane needs to be spanned, such as in the chloroplast or mitochondria, meaningful rates are possible only if several intervening cofactors are involved. This is why all transmembrane redox complexes use multiple cofactors.

As we have seen, photosynthetic systems are highly constrained. Electron transfer rates must be achieved that exceed the 10^{-8} s limit imposed on the excited state of the sensitizer by fluorescence. Given a 99% quantum yield, electron transfer rates must exceed 10^{-01} s. This can only be accomplished by placing the primary electron acceptor a very short distance from the excited sensitizer in the initial stage of charge separation.

If we look at the placement of cofactors in the bacterial reaction center, we see that this condition is met. Looking back to Figure 7, we see that the distance between the bacteriochlorophyll special pair, P_{865}, and the bridging bacteriochlorophyll is ca. 6 Å, and the distance between the bridging bacteriochlorophyll and the primary acceptor bacteriopheophytin *a*, BPh, is ca. 5 Å. The rate of electron transfer between P_{865} and BPh has been measured to be 2.8 ps, which corresponds roughly to the sum of the optimal rates of electron between these three components. The distance between BPh and Q_A is 10 Å and the electron transfer rate is 200 ps, which again is roughly in line with the 1 ns time predicted in Figure 11.

Thus, the reason for the need for the earliest steps of electron transfer to be faster than 10^{-8} s is accomplished by placing the electron transfer cofactors in exceedingly close contact. No other multicofactor enzyme, to my knowledge, places cofactors at these close distances.

Problem 5. Using the relationship between optimal rates and edge-to-edge distance for of long-distance electron transfer in proteins, calculate how many electron transfer cofactors would be needed to span a 40 Å thick biological membrane in a time period of 10 μs. Assume for the purpose of this argument each cofactor is a transition metal with a radius of 1.5 Å.

The question arises whether there is a role for the Franck-Condon factor in photosynthetic electron transfer. It is true that each step is accomplished with a drop in Gibbs free energy, but this may simply be to ensure that the equilibrium is biased toward product formation. However, each forward electron transfer step also competes with an inherent charge recombination step.

For example, P_{865}^{+} recombines with Q_A^{-} with a half-time of about 100 ms. The $-\Delta G^{o}$ is very large for this reaction, and this may have the otherwise-paradoxical effect of pushing the reaction into the 'inverted' Marcus region. This would tend to slow down the charge recombination rate, thereby further guaranteeing that forward electron transfer remains highly efficient. Whether this actually happens in any known photochemical reaction center, however, is still the topic of discussion.

3.5. Photosystem II: a variation on a theme of the bacterial reaction center.

We will now examine the components and electron transfer process in Photosystem II.

3.5.1. Details of Quinone-Type Reaction Centers: Photosystem II

The purple bacterial reaction center shares a striking similarity to Photosystem II of plants and cyanobacteria. Electron transfer on the acceptor side is virtually identical in that plastoquinone (see Figure 4) is reduced to dihydroplastoquinol at the Q_B site (Figure 12), which subsequently leaves the binding site to interact with the cytochrome b_6f complex. An oxidized plastoquinone that has returned from the cytochrome b_6f reoccupies the Q_B site for another round of light-induced reduction. Because the tertiary acceptor is a mobile quinone, both the bacterial reaction center and Photosystem II are termed 'Type II' reaction centers.

The location of polypeptides in the 3.8 Å X-ray crystal structure of Photosystem II (PDB entry 1FE1) is depicted in Figure 12. Note the presence of the five core transmembrane □-helices A through E on the D1 and D2 proteins that together comprise the heterodimer, and the presence of six □-helices on CP43 and CP47 that comprise the antenna proteins. It is interesting that the D1/D2 heterodimeric proteins of Photosystem II overlay almost perfectly the core heterodimeric proteins of the bacterial reaction center.

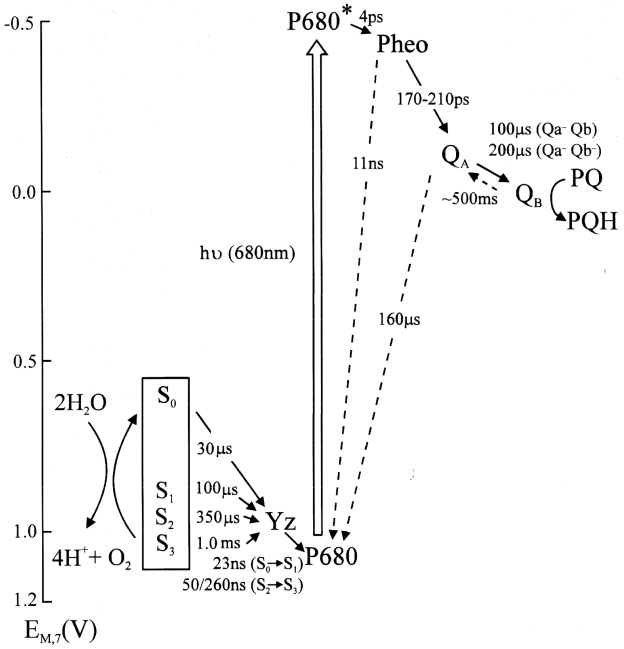

Figure 12. The components of the Photosystem II reaction center depicted with redox potential on the y-axis and rate of electron transfer on the x-axis. Note the similarity in the identity of the cofactors and the electron transfer rates with the bacterial reaction center.

Nonetheless, electron transfer on the oxidizing side is different from the bacterial reaction center in that the primary electron donor, P680, has a redox potential in excess of +1V, and a Mn_4 cluster exists that oxidizes two water molecules to dioxygen in a reaction that requires four photons. A redox-active tyrosine (Y_Z) links $P680^{+}$ to the Mn_4 cluster and, in cooperation with a nearby histidine residue, participates in moving the released protons to the aqueous phase. The details of the Mn_4 cluster and the chemistry of water oxidation are not well understood. A model of the Mn_4 water-oxidizing cluster is depicted in Figure 14 superimposed on the 3.5 Å electron density map of Photosystem II (Zouni et al. 2001). Because of the oxidation of water and the release of dioxygen, the Photosystem II reaction

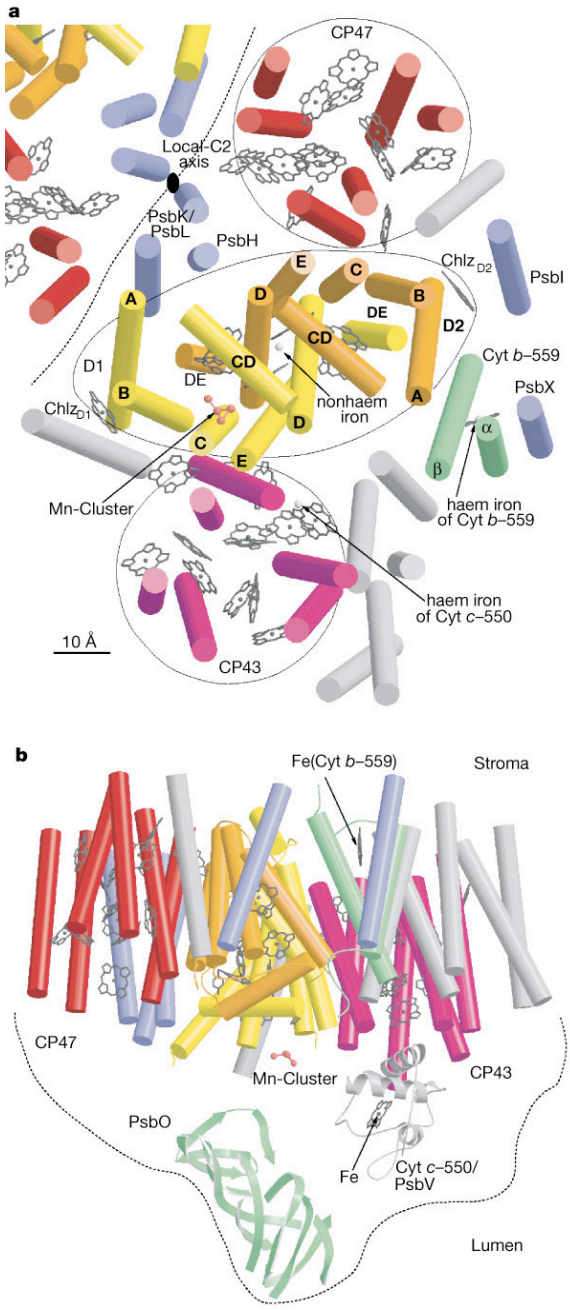

Figure 13. Model for Photosystem II from Synechococcus elongatus based on the X-ray crystal structure at 3.8 Å. a) Top view from the lumenal side showing polypeptides A through E on D1 and D2, the reaction center core proteins. Also depicted are the peripheral antenna proteins CP43 and CP47, each of which consists of six membrane spanning a-helices. b) Side view showing the membrane-spanning subunits as well as the Mn cluster, the PsbO protein and the bound cytochrome. Reproduced with permission from Zouni et al., 2001; http://www.nature.com/

,

center does not operate in a cycle as does the bacterial reaction center. Rather, the released protons from water oxidation are deposited on one side of the thylakoid membrane to help build the electrochemical gradient.

The electrons derived from water pass through the cytochrome b_6f complex and find their way to Photosystem I via a small, copper-containing protein named plastocyanin (under copper-limiting conditions, cytochrome c_6 can substitute for plastocyanin in certain cyanobacteria and algae). Photosystem I ultimately promotes these electrons to a reduction level sufficient to reduce $NADP^+$. The electron transfer pathway in plants and cyanobacteria is hence linear, with Photosystem II and Photosystem I operating in series.

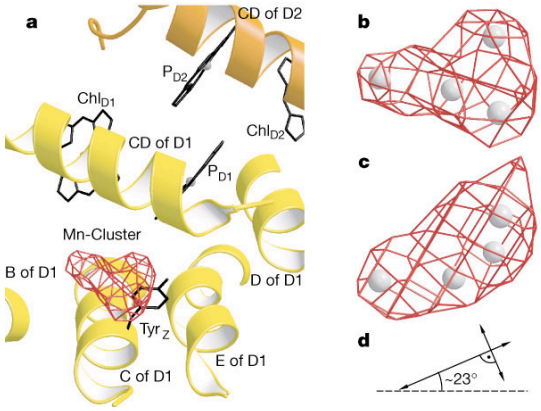

Figure 14. Model for the Mn_4 cluster in Photosystem II from Synechoccus elongatus based on the 3.8 Å x-ray crystal structure and on EXAFS data. Reproduced with permission from Zouni et al., 2001; http://www.nature.com/

Take home message #7: In higher plant, algal and cyanobacterial photosynthesis, Photosystem II functions as a non-cyclic photochemical reaction center, removing electrons from water and transferring them through the cytochrome b_6f complex to Photosystem I, which ultimately reduces $NADP^+$.

3.6. Photosystem I: Structure, Function and Organization of Cofactors and Proteins.

With the description of Marcus theory and Type II reaction centers as background, we now move to an analysis of Photosystem I.

3.6.1. Details of Photosystem I: General Overview

Photosystem I shares many common features with Type II reaction centers. In particular, a protein heterodimer consisting of PsaA and PsaB comprises the heart of the reaction center. The electron transfer cofactors include a pair of chlorophyll *a* molecules as the primary electron donor, a chlorophyll *a* monomer as the primary electron acceptor, and a phylloquinone (2-methyl-3-phytyl-1,4-naphthoquinone) as a secondary electron acceptor (see Figure 4). Two molecules of phylloquinone exist per reaction center, but whether one or both are active in transferring electrons is still under investigation.

The differences with Type II reaction centers exist primarily on the electron acceptor side. Photosystem I utilizes a [4Fe-4S] cluster that, unlike the non-heme iron in the bacterial reaction center, functions in electron transfer. This interpolypeptide [4Fe-4S] cluster is a rather uncommon motif, found in the nitrogenase Fe protein and in only a few other proteins. Its purpose is to intercept the electron from the singly reduced phylloquinone and vector it toward the stromal (cytoplasmic) phase.

Two additional [4Fe-4S] clusters, termed F_A and F_B, participate in this process by providing a pathway for electrons to leave the reaction center. These clusters are bound to a stromal-bound polypeptide labeled PsaC. The electrons are picked up by the soluble [2Fe-2S] protein, ferredoxin, a one-electron carrier protein, which can in turn form a complex with ferredoxin :$NADP^+$ oxidoreductase to reduce $NADP^+$ to NADPH. The latter enzyme can be thought of as a 1-electron, 2-electron accumulator. Photosystem I is termed a 'Type I' reaction center due to the presence of iron-sulfur clusters as electron acceptors.

3.6.2. Details of Photosystem I: the Pre-Crystal Model

Cyanobacterial Photosystem I was known from biochemical and genetic studies (Golbeck, 1994) to consist of 11 subunits (an additional subunit was discovered in the high-resolution x-ray crystal structure.) A cartoon of the cyanobacterial reaction center, which was assembled prior to the crystal structure from biochemical, spectroscopic and genetic evidence (Golbeck 1992), is depicted in Figure 15.

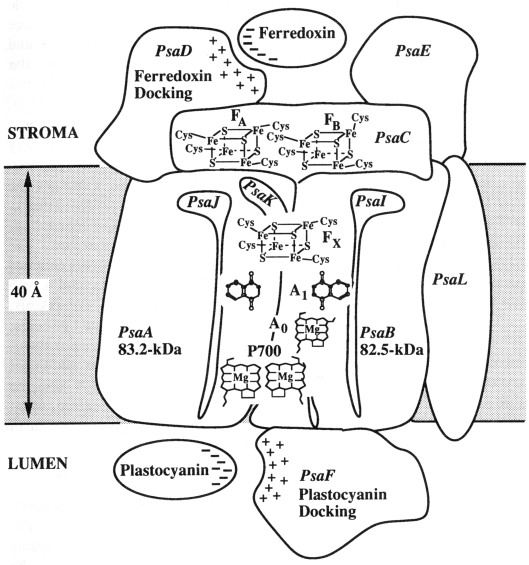

Figure 15. *Pre-crystal cartoon of Photosystem I based on spectroscopic, biochemical and genetic evidence. P700 was shown to be a chlorophyll a special pair by EPR; F_X was found to be an interpolypeptide cluster by EPR and biochemical studies; two phylloquinones were known from chemical extraction; and PsaC, PsaD and PsaE were deduced to be stromal proteins from biochemical studies. With permission, from the Annual Review of Plant Physiology and Plant Molecular Biology, Volume 43 © 1992 by Annual Reviews; www.annualreviews.org*

The primary electron transfer cofactors were proposed to be located on the PsaA and PsaB polypeptides, which form a heterodimer, and on the peripheral PsaC

protein, which is similar to a small, dicluster bacterial ferredoxins. Two other peripheral proteins, PsaD and PsaE were also found to be located on the stromal ridge along with PsaC. The function of PsaD and PsaE is to assist in docking ferredoxin, and an additional function of PsaE may be to regulate cyclic electron transfer around Photosystem I. The function of PsaF is related to plastocyanin docking, at least in algal and higher plant Photosystem I.

The assembly of the stromal Photosystem I subunits is known from resolution and reconstitution studies (Golbeck, 1995): the F_X iron-sulfur cluster and the F_A/F_B clusters must be present for PsaC to bind, and PsaC must be present for PsaD and PsaE to bind. The assembly of F_X, in turn, requires the participation of a membrane-bound rubredoxin (Shen et al. 2002). This orderly assembly probably ensures that the three stromal subunits do not bind to PsaA/PsaB heterodimers that lack F_X.

One interesting detail is that Photosystem I is isolated from cyanobacterial membranes as a trimer, whereas it is isolated from higher plant membranes as a monomer. The deletion of PsaL in cyanobacteria results in the isolation of monomers, but functions for the other low-molecular mass subunits could not be definitively be assigned due to a lack of a phenotype in other mutants.

3.6.3. Details of Photosystem I: High-Resolution EM and Crystallization Efforts

High-resolution transmission electron microscopic images provided the first visual depiction of the Photosystem I reaction center. In this technique, thousands of high-resolution electron micrographs are selected and averaged, thereby allowing the general contours of membrane proteins to be visualized (Boekema et al. 1987).

The images showed clearly the trimeric nature of cyanobacterial Photosystem I (Figure 16). The trimers are shaped as a disk with a radius of 105 Å and a thickness of 65 Å (not including the 'stromal ridge', which would add another ca. 30 Å), and the monomers within the trimer are asymmetrical. The images showed three prominent 'bumps' on the stromal surface of each monomer that, from biochemical resolution and reconstitution studies, were thought to represent the three stromal proteins. Images constructed from deletion mutants, allowed the unambiguous identification of PsaC, PsaD and PsaE. The remaining 9 polypeptides, including PsaA and PsaB, are integral membrane-spanning subunits of Photosystem I.

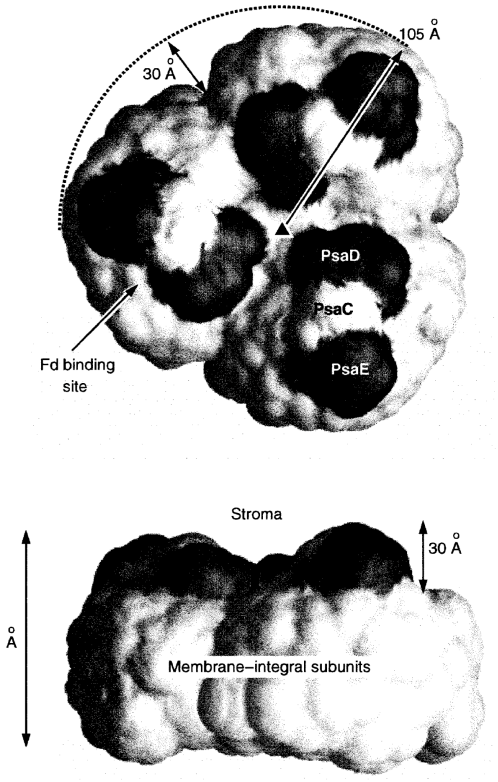

Figure 16. High-resolution electron microscopic images of Photosystem I. The figure represents 1970 top views and 457 side views that were selected from electron micrographs and subsequently aligned to different references. The classification shows that the Photosystem I trimeric complex consists of three very similar, if not identical, units. Reprinted from Biochim. Biophys. Acta, 974, Boekema EJ, Dekker JP, Rögner M, Witt I, Witt HT, Van Heel M. 'Refined analysis of the trimeric structure of the isolated photosystem I complex from the thermophilic cyanobacterium Synechococcus sp', *pp. 81-87. Copyright (1989) with permission from Elsevier.*

At about the same period in time, Photosystem I was reported crystallized from the oxygenic cyanobacterium *Synechococcus elongatus* (Witt et al. 1987). During the 12 years that elapsed from this first report of crystals to the atomic model at 2.5 Å resolution, intermediate models were constructed from electron density maps at resolutions of 6 Å and 4 Å.

As we will see in the next several sections, a wealth of information could be obtained from these intermediate models. The crystals were photochemically active, and the high water content allowed the diffusion of reductants and oxidants, a necessary precondition for magnetic resonance and optical spectroscopic studies.

3.6.4. Details of Photosystem I: X-Ray Crystallography at 6 Å Resolution

The unit cell in the Photosystem I crystals (Krauß et al. 1993) contains two trimers as shown in Figure 17. The crystals are ca. 80% water, and the crystal contacts involve only a very few amino acids, occurring primarily between PsaE on the stromal side of one Photosystem I trimer and PsaF on the lumenal side of another Photosystem I trimer.

The key to the interpretation of the 6 Å electron density map lies in the presence of the three iron-sulfur clusters. Due to their extremely high electron density, F_X, F_B and F_A were readily located, and nearby were six regions of electron density that resembled the six chlorophyll *a* molecules involved in electron transfer in the bacterial reaction center.

This was the first indication that bridging chlorophylls were present between the primary donor (P700) and the primary acceptor (A_0) chlorophylls. Thus, the basic photochemical motif of six chlorophylls was found to be conserved between the bacterial reaction center and Photosystem I. A total of 28 □-helices and 45 chlorophyll *a* molecules were located in the 6 Å map, with the PsaA/PsaB heterodimer represented by nine □-helices.

The interpolypeptide location of F_X that was proposed from biochemical and EPR studies was confirmed, and a pseudo C_2 axis of symmetry was found to run through P700 and the F_X cluster. The big surprise, however, was that the vector that connects F_A and F_B is tilted at an angle of ca. 62° from the membrane normal. Thus, the stromal PsaC protein is tilted away from the membrane plane, a geometry that breaks the C_2 axis of symmetry of the reaction center as a whole. One important implication from this finding is that because of the distances involved, electron transfer must be must occur serially through the three iron-sulfur clusters.

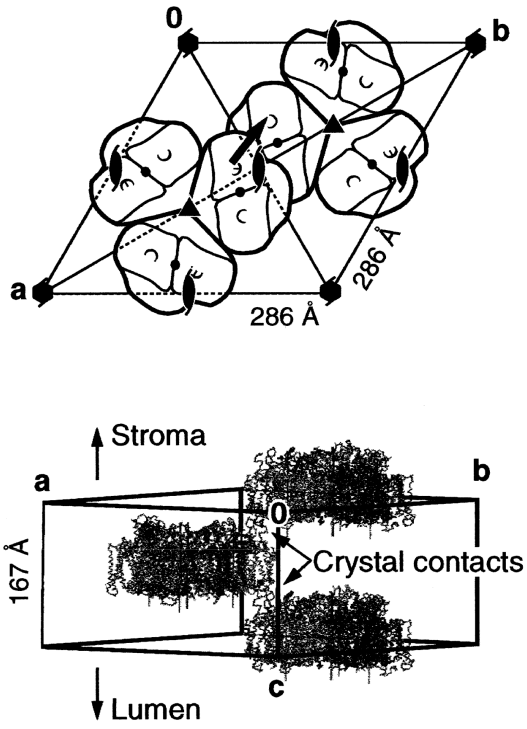

Figure 17. Schematic view of the unit cell and the packing scheme of Photosystem I trimers. Reprinted from J Mol Biol 272, Schubert WD, Klukas O, Krauß N, Saenger W, Fromme P, Witt HT. 'Photosystem I of Synechococcus elongatus *at 4 Å resolution: comprehensive structure analysis', pp. 741-769. Copyright (1997), with permission from Elsevier.*

Problem 6. The center-to-center distance between F_X and the closest iron-sulfur cluster in PsaC (F_A) is 14.9 Å, between F_X and the most distant iron-sulfur cluster in PsaC is 22 Å between F_A the F_B is 12.3 Å (see Figure 15). Show why electron transfer must occur serially through the three iron-sulfur clusters.

3.6.5. Details of Photosystem I: X-Ray Crystallography at 4 Å

In the 4 Å electron density map of Photosystem I (PDB entry 1C51), nearly all of the transmembrane a-helices could be identified and the positions of ca. 80 of the 96 total chlorophyll *a* antenna molecules could be located (Schubert et al. 1997). Because the side chains of the amino acids could not be resolved at this resolution (Figure 18), the membrane-spanning subunits were assigned indirectly.

For example, the identification of PsaF, PsaI, PsaJ, PsaK, PsaL and PsaM was aided by prior biochemical studies, including chemical cross-linking to identify nearest neighbors, proteolysis and biotinylation studies to identify surface-exposed subunits, and mutagenesis studies to determine susceptibility of the subunits to detergents and chaotropic agents (Chitnis 2001). Through these techniques, the following polypeptides were found to be neighbors: PsaE/PsaF/PsaJ; and PsaL/PsaI. Due to its size and hydrophobicity, PsaK was predicted to span the membrane twice, and a PsaL deletion mutant formed only monomers, allowing it to be localized near the C_3 symmetry axis.

PsaD and PsaE were long known to be stromal subunits, and PsaC contains the two iron-sulfur clusters, F_A and F_B. Only the PsaM subunit was assigned by default. One interesting finding was that surface-located α-helices present on PsaA and on PsaB are comparable to the surface α-helices present in the bacterial reaction center. The significance of these α-helices will become apparent shortly. The phylloquinones were not identified on this electron density map, which was not unexpected because at this resolution they also resemble the side chains of bulky amino acids.

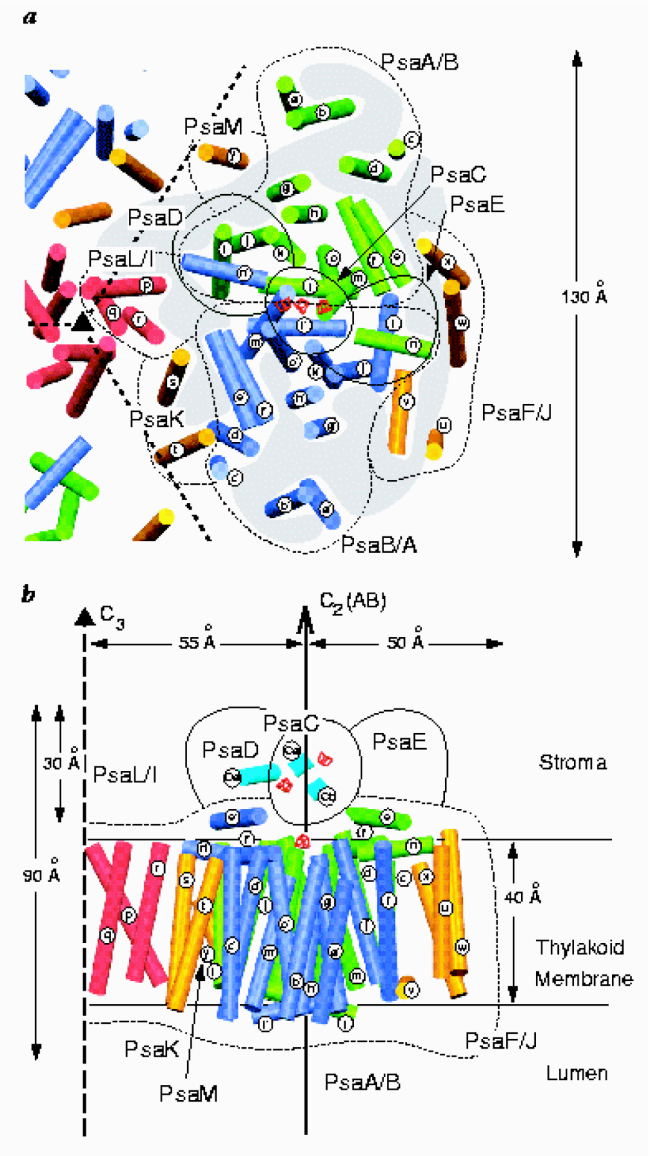

Figure 18. Cartoon of Photosystem I at 4 Å resolution. a) top view from the stromal side, b) side view. The blue and green colors represent the heterodimer PsaA/PsaB (not identified at this resolution). The surface α-helices (n and n') are visible as are the core polypeptides i(i'), j(j'), k(k'), l(l') and m(m'). The α-helical part of PsaD is depicted, as are the two small α-helical regions of PsaC. Reproduced with permission from Krauß et al., 1996; http://www.nature.com/

Electron paramagnetic resonance (EPR) spectroscopy (see appendix in Ohnishi et al. 1998 for a short explanation of EPR) proved especially valuable in providing structural information that supplemented the 4 Å model of Photosystem I. In particular, the distance between $P700^+$ and the phylloquinone anion radical, A_1^-, was found to be 25.4 Å by measuring the dipolar coupling between the two spin systems, and the orientation of the dipolar coupling axis with respect to the crystallographic axes (*i.e.* the tilt angle of the P700-A_1 axis relative to the membrane normal) was determined by measuring the angular dependence of the dipolar coupling in single crystals of Photosystem I (Bittl and Zech 2001).

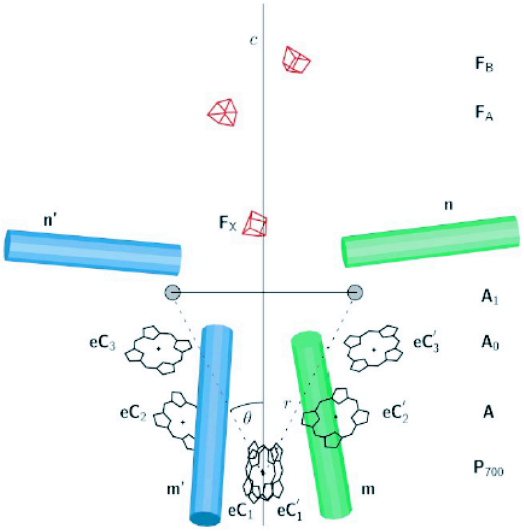

Figure 19. Electron paramagnetic resonance spectroscopy was the first structural technique to provide information on the location of the phylloquinones in Photosystem I. The position of the quinones (grey circles) is superimposed on the 4 Å model of the Photosystem I, showing the transmembrane m (m') helix which provides the ligands for P700, and the surface-located n (n') helix, which was thought to bind the quinone. The experimental parameters obtained of distance (r) and angle (f) define a circle, which when superimposed on the low-resolution model of PS I, provided a highly plausible location for the phylloquinones. The location was later verified in the high-resolution 2.5 Å model of Photosystem I. Reprinted from Biochim Biophys Acta 1507, Bittl R, Zech SG. 'Pulsed EPR spectroscopy on short-lived intermediates in Photosystem I', pp. 194-211. Copyright (2001), with permission from Elsevier.

The distance and angle measurements define a circle, and when this circle is superimposed on the 4 Å model of Photosystem I, the quinones can be located at the intersection of the membrane-spanning m/m' □-helices and the surface n/n' □-helices mentioned above (Figure 19). It is interesting that Q_A and Q_B exist in roughly the same relative locations in the bacterial reaction center, at the intersection of a membrane-spanning □-helix and a surface □-helix.

Independently, the three-dimensional structures of unbound PsaC, PsaD and PsaE were probed by NMR spectroscopy (Figure 20). PsaC (PDB entry 1K0T) was found to be folded in a manner similar to that of low molecular weight dicluster ferredoxins (Antonkine et al. 2002). Both iron-sulfur cluster binding motifs and clusters exhibit a local pseudo-C_2-symmetry, which also applies but to a lesser extent to other regions of the protein. PsaC differs from dicluster ferredoxins, however, in three regions: a minor 2-residue extension of the N-terminus, a sequence insertion of 8 residues in the middle of the loop connecting the two consensus iron-sulfur binding motifs, and a C-terminal extension of 15 residues.

PsaD exists as a dimer in solution and has at least two domains, one structured and the remainder unstructured (Xia et al. 1998). The structured domain contains a small amount of □-sheet. It is likely that PsaD falls into the category of a 'natively unstructured' protein because it assumes it final 3-dimensional shape only when bound to Photosystem I.

PsaE (PDB entries 1PSF, 1QP2) was found to consist of a five-stranded □-sheet with (+1, +1, +1, -4x) topology and a single turn of a 3(10) helix between the □ D and □ E strands (Falzone et al. 1994). Interestingly, a portion of the structure is similar to the Src homology 3 (SH3) domain, a motif found in membrane-associated proteins involved in signal transduction in eukaryotic organisms.

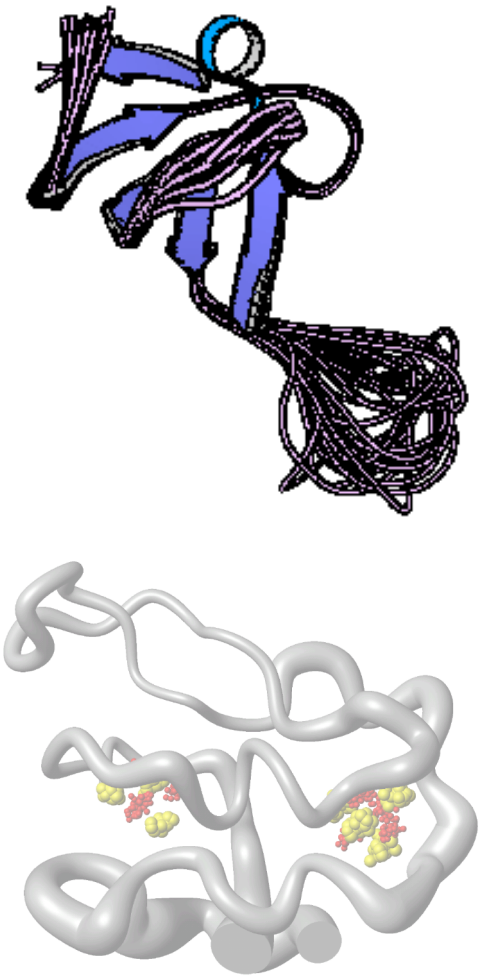

Figure 20. NMR solution structure of unbound PsaE (PDB entry 1QP2) and PsaC (PDB entry 1K0T). (Top) Ribbon diagram of the lowest energy structure of PsaE from Nostoc sp. PCC 8009. The protein is a 5-stranded 3_{10} b-sheet sheet with an a-helical turn between the pentultimate and last strands. (Bottom) Sausage diagram of PsaC constructed from 30 energy-minimized structures. The iron atoms are shown in red and the labile sulfides are shown in yellow; the N- and C-termini are truncated for clarity. PsaE courtesy of Juliette Lecomte. PsaC from J Biol Inorg Chem 'Solution structure of the unbound, oxidized Photosystem I subunit PsaC, containing [4Fe-4S] clusters F_A and F_B: a conformational change occurs upon binding to Photosystem I', Antonkine ML, Liu G, Bentrop D, Bryant DA, Bertini I, Luchinat C, Golbeck JH, Stehlik D., vol. 7, pp. 461-472, Figure 7, 2002; © Springer.

With the publication of the 4 Å model of Photosystem I, a new symmetry-related issue arose: the orientation of PsaC relative to the axis that connects the two iron-sulfur clusters. The consequence of the local pseudo-C_2-symmetry in PsaC mentioned above is that its orientation on the Photosystem I core is ambiguous on a low-resolution electron density map. The orientation of PsaC could, in principle, be determined on a high-resolution electron density map of Photosystem I due to the non-symmetry related elements in PsaC, such as the internal loop and the extended C-terminus.

However, the resolution of the 4 Å map was insufficient to reveal these details, and the orientation of PsaC was ultimately solved using biochemical and biophysical techniques (Golbeck 2001). In the end, it was shown that the cluster nearest to F_X is F_A and the cluster nearest to the stromal surface is F_B. Since the location of F_A and F_B relative to the protein axis was known from earlier mutagenesis and electron paramagnetic resonances studies (Zhao et al. 1992), the overall orientation of PsaC could be determined without ambiguity. Given the midpoint potentials of F_A (-520 mV) and F_B (-580 mV), this orientation implies that a small thermodynamically uphill electron transfer step is associated with the terminal electron acceptors.

3.6.6. Details of Photosystem I: Cofactor Arrangement at Atomic Resolution

The 2.5 Å atomic resolution X-ray crystal structure of Photosystem I (PDB entry 1JB0) (Jordan et al. 2001) finally revealed the location of 12 polypeptides, 96 chlorophylls, 2 phylloquinones, three [4Fe-4S] clusters, 22 carotenoids, 4 lipids and 1 Ca^{2+} molecule (Figure 21). The presence of the 4 lipids came as a surprise; they appear to be an integral part of the structure and not just a contaminant from isolation. Their function is at this time unknown. At this resolution, the non-symmetry related elements are visible in PsaC, confirming its orientation such that F_A is proximal to F_X and F_B is proximal to the ferredoxin binding site.

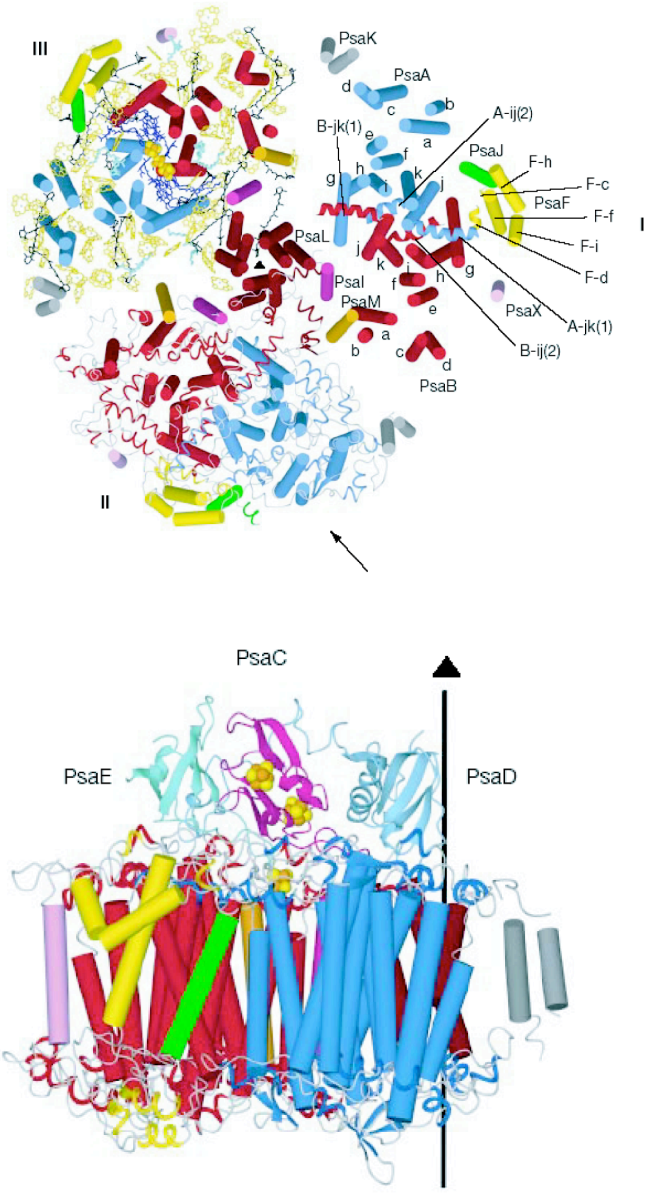

Figure 21. a) Top view and b) end view of the Photosystem I reaction center (PDB entry 1JB0) showing the C_3 axis of symmetry (arrow). The reaction center polypeptides are largely membrane-intrinsic a-helices consisting of PsaA and PsaB (red and blue), PsaF (yellow), PsaL (grey), PsaM (pink) and three stromal proteins, PsaC (magenta), PsaD (blue) and PsaE (cyan). The thickness of the biological membrane can be estimated from the height of the membrane-spanning helices. The electron transfer cofactors from P700 to F_X are embedded within the membrane phase and thereby shielded from the solvent. Photosystem I exists in the membrane of cyanobacteria as a trimer. Reproduced with permission from Jordan et al., 2001; http://www.nature.com/

There exist significant differences in structure with the unbound form of PsaC, primarily in the arrangement of the N- and C-termini with respect to the [4Fe-4S] core domain (Antonkine et al. 2003). These changes are thought to be important in the process of binding to the Photosystem I core (Figure 22). The N-terminal, □-sheet that represents the core portion of PsaD is firmly bound to PsaA and PsaB, but a long, extended arm of the a 'C-clamp' reaches over the surface of PsaC and attaches itself via the C- terminus, to PsaB (Figure 21). It is a remarkable feature; its presence may lock the correct PsaC orientation with respect to the PsaA and PsaB heterodimer; it also induces conformational changes in PsaC, thereby establishing the magnetic properties of F_A and F_B observed in the wild-type complex, allowing for the efficient reduction of ferredoxin. In contrast, PsaE has nearly the same conformation in the unbound state as in the bound state, and appears to have little effect on the properties of the iron-sulfur clusters in PsaC.

The atomic resolution structure showed that P700 is a heterodimer, consisting of a chlorophyll *a'* (the 13' epimer of chlorophyll *a*) ligated to the PsaA subunit via an axial histidine nitrogen to the central Mg^{2+} atom, and a chlorophyll *a* ligated to the PsaB subunit via an axial histidine nitrogen to the central Mg^{2+} atom (Figure 23). The existence of a chlorophyll *a'* as a component of P700 had been predicted from earlier chemical extraction studies (Watanabe et al. 1985). There are three H-bonds to the chlorophyll *a'* molecule, which are thought to aid in its selective insertion into the PsaA polypeptide, but which also break the otherwise nearly perfect symmetry of the electron transfer cofactor chain.

On both branches, a water molecule serves as the axial ligand to the bridging chlorophyll *a* molecules and surprisingly, a methionine sulfur is the axial ligand to the primary acceptor chlorophyll *a* molecules. This is the first reported instance of a sulfur ether as a ligand to a chlorophyll molecule.

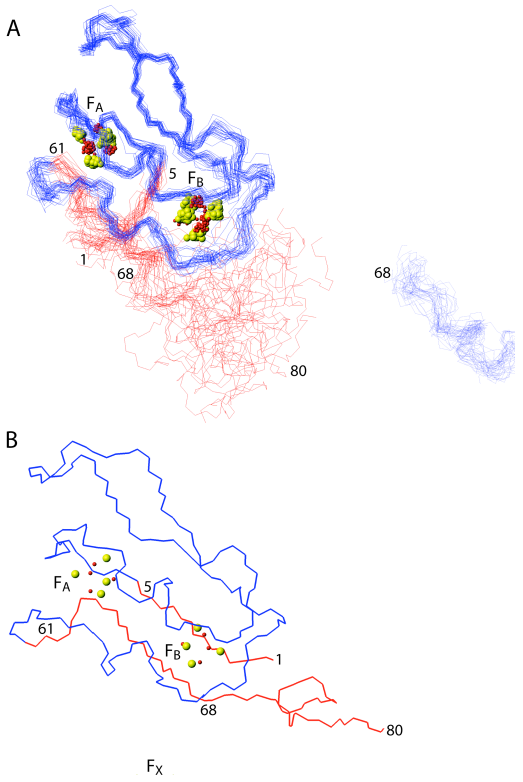

Figure 22. Comparison of 30 superimposed NMR solution structures of unbound PsaC (A) with the X-ray crystal structure of bound PsaC (B). The regions where the two structures show significant differences are identified in red. The inset in (A) represents a superposition based on residues 68 to 80, and indicate a helical secondary structure of the C-terminus. J Mol Biol 327, Antonkine ML, Jordan P, Fromme P, Krauß N, Golbeck J, Stehlik, D. 'Assembly of protein subunits within the stromal ridge of Photosystem I. Structural changes between unbound and sequentially-bound PS I-bound polypeptides and correlated changes of the magnetic properties of the terminal clusters', pp. 671-697. Copyright (2003), with permission from Elsevier.

The phylloquinones were found where they had been predicted to be from the magnetic resonances studies. On both branches, the phylloquinones are bound to the protein via an H-bond from the peptide backbone of a leucine to the oxygen *ortho* to the phytyl tail on the quinone, and there is a tryptophan residue in contact with the phylloquinone.

The presence of a bifurcating electron transfer chain on the PsaA-side and PsaB-side (Figure 23) begs the question whether electron transfer in Photosystem I is bidirectional or unidirectional (as in the bacterial reaction center). There is no inherent requirement for unidirectional electron transfer, because unlike Type II reaction centers, both quinones in Type I reaction centers remain bound and either or both can, in principle, function exclusively as a one-electron redox cofactor. However, there exist subtle differences in the distances and geometries of the electron transfer cofactors on the PsaA-branch and the PsaB-branch, and this makes it exceedingly unlikely that electron transfer is precisely equivalent along both sides.

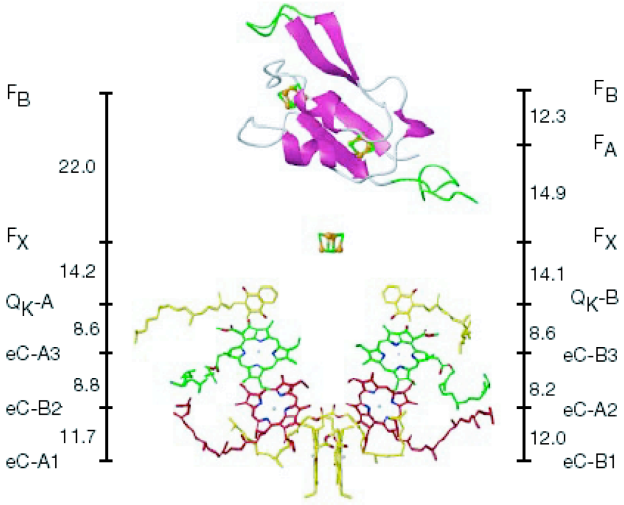

Figure 23. The arrangement of electron transfer cofactors and the center-to-center distances. Note the bifurcating electron transfer pathway that diverges at P700 (eC-A1 and eC-B1) and converges at the interpolypeptide F_X iron-sulfur cluster. In cyanobacteria, the electron transfer pathway is known to proceed up the PsaA-bound cofactors (eC-A3 and Q_K-A) but whether the PsaB-side cofactors (eC-B3 and Q_K-B) support substantial electron transfer is still under investigation. The bridging chlorophyll on the PsaA chain is ligated through a water by a PsaB-side residue, and the the bridging chlorophyll on the PsaB chain is ligated through a water by a PsaA-side residue. The electron is handed transferred from F_X through F_A and F_B to soluble ferredoxin. Note the high degree of similarity in P700 through Q_K-A and Q_K-B in Photosystem I with P865 through Q_A and Q_B in the bacterial reaction center. Reproduced with permission from Jordan et al., 2001; http://www.nature.com/

Problem 7. Download the file 1JBO from the protein database. Locate the main structural features of the Photosystem I reaction center that are responsible (i) for its ability to transfer electrons across the membrane and to reduce ferredoxin, (ii) for the stability of the PsaA/PsaB dimer, and (iii) for the binding of the stromal polypeptides PsaC, PsaD and PsaE. (ii) Identify the role of key amino acids.

3.6.7. Details of Photosystem I: Electron Transfer Rates

The forward and backward electron transfer rates for Photosystem I are depicted in Figure 24. Electron transfer from A_0 to A_1 occurs with a lifetime of ca. 20 ps, (Hastings et al. 1994), which is similar to the lifetime of the primary acceptor in the bacterial reaction center. This lifetime is also consistent with the distances between the primary electron donor and acceptor.

Electron transfer from A_1 to F_X is biphasic, with lifetimes of ca. 20 ns and 200 ns (Sétif and Brettel 1993). The reason for the biphasic electron transfer kinetics is unclear. One possibility is that one kinetic phase represents electron transfer up the PsaA-side cofactors while the other kinetic phase represents electron transfer up the PsaB-side cofactors (Joliot and Joliot 1999). Another possibility is that both kinetic phases represent unidirectional electron transfer among phylloquinones in two slightly different environments The only certainty at this time is the PsaA-side phylloquinone is active in electron transfer (Boudreaux et al. 2001; Yang et al. 1998).

The electron transfer rates between F_X, F_B and F_A are not known with certainty; however, the electron reaches ferredoxin in 500 ns (Sétif and Bottin 1994). Because of the distances involved, it is also likely that the electron transfer step between F_A and F_B is faster than the step between F_X and F_A. The remaining reactions involve solution biochemistry; the electron is transferred from F_B to soluble ferredoxin, which in turn interacts with ferredoxin:$NADP^+$ oxido-reductase to reduce $NADP^+$ to NADPH.

Meanwhile, plastocyanin or cytochrome c_6 reduces $P700^+$ using an electron taken from the cytochrome b_6f complex, thereby returning Photosystem I to its initial state and poising it for another round of light-induced turnover. Thus, Photosystem I is an enzyme that can be classified as a light-driven, plastocyanin:ferredoxin oxido-reductase.

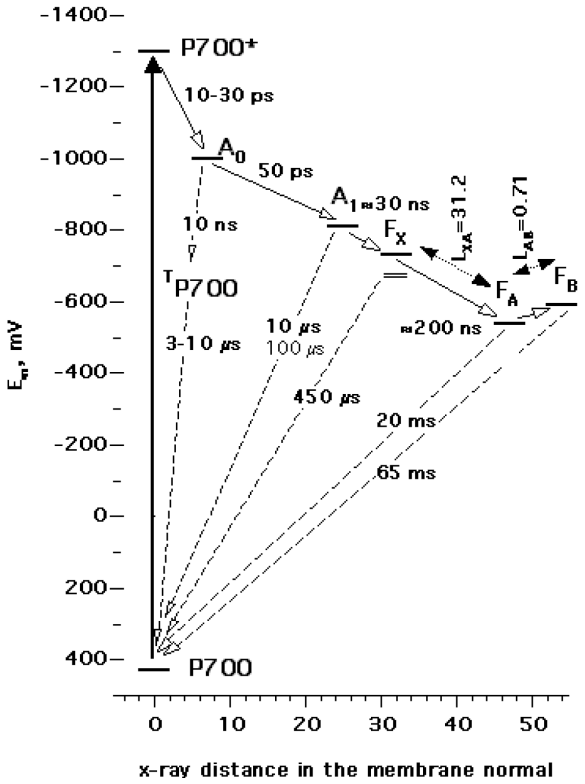

Figure 24. Plot of the midpoint potential vs x-ray distance in the membrane normal for the electron transfer cofactors in Photosystem I. The forward electron transfer rates are shown along with the charge recombination rates. Note that the forward rates are usually three orders of magnitude faster than the backward rates, thereby ensuring a high quantum yield in Photosystem I. The equilibrium constants are also depicted here. Reproduced from Biochim Biophys Acta 1507, Vassiliev IR, Antonkine ML, Golbeck JH. 'Iron-sulfur clusters in type I reaction centers', pp. 139-160. Copyright (2001), with permission from Elsevier.

Problem 8. How much energy, in eV and kJ, is stored at pH 7 in reducing equivalents when two electrons are transferred from the special pair of Photosystem I (E_m = +430 mV) to the primary quinone, A_1, whose E_m 7 is -800 mV?

3.6.8. Details of Photosystem I: Arrangement of the Antenna Chlorophylls

In addition to the six chlorophyll *a* molecules that are proposed to serve an electron transfer function, there exist 90 additional chlorophyll *a* molecules that serve as antenna. Their function is to increase the optical cross-section by feeding excitons to the trapping center, P700. The reason for the existence of antenna chlorophylls is that the solar flux is insufficient to excite the trapping chlorophyll, P700, at rates comparable with the maximum throughput ca. 1000 electrons second in Photosystem I. Were the antenna to be absent, and only the six photoactive chlorophylls to function as antenna, then the solar flux would still be limited to promoting a very sub-marginal electron transfer rate (See Problem 9).

In principle, the plant or cyanobacterium could compensate by increasing the number of reaction centers per unit area. However, this would be undesirable if only because iron, in particular, is difficult to assimilate (it is present in the environment as the highly-insoluble oxide) and the synthesis of protein is metabolically expensive.

It makes more biophysical and biochemical sense simply to increase the number of metabolically inexpensive chromophores and place them close together in a protein environment in which they can rapidly transfer the exciton among themselves, and ultimately to the trapping center, P700. This is the same principle used by parabolic dish antennas for the reception of microwaves; the dish focuses the electromagnetic radiation on a single active transistor that converts the concentrated radio waves to an electric current. This is a lot cheaper than ganging hundreds or thousands of transistors together in an array to detect the weak radiation field.

As in most reaction centers, the Photosystem I chlorophylls are not all in the same environment. This leads in a distribution of spectral maxima and to a correspondingly broader absorption range for visible quanta. Most of the chlorophylls are bound to the PsaA/PsaB heterodimer, but each of the small membrane-spanning polypeptides (PsaF, PsaI, PsaJ, PsaK, PsaL, PsaM and PsaX) binds from one to four antenna chlorophyll molecules. Thus, the small, membrane-spanning polypeptides are antenna chlorophyll proteins, a function that would not have been uncovered easily through deletion mutagenesis studies.

The six N-terminal □-helices in Photosystem I can be thought of as an accessory chlorophyll protein that is covalently bound to the reaction center protein. When observed from the side, the antenna chlorophylls are found to be distributed in two rings (Figure 25), with one ring near the stromal side and the other ring near the lumenal side of the membrane. Two of the antenna chlorophylls are positioned between the antenna ring and the photoactive chlorophylls. It is thought that they provide a pathway for exciton transfer between the antenna bed and the reaction center core pigments.

There are also 22 □-carotene molecules that probably serve protective as well as antenna functions in the reaction center. A triplet state on a chlorophyll *a* can be transferred to a □-carotene and then converted harmlessly to vibrational motion (heat) through internal conversion. Here it is perhaps significant that □□carotene molecules do *not* fluoresce strongly; thus, the energy is dumped to heat very quickly. It is also significant that every photochemical reaction center and nearly every antenna chlorophyll protein has □-carotene embedded throughout their structures.

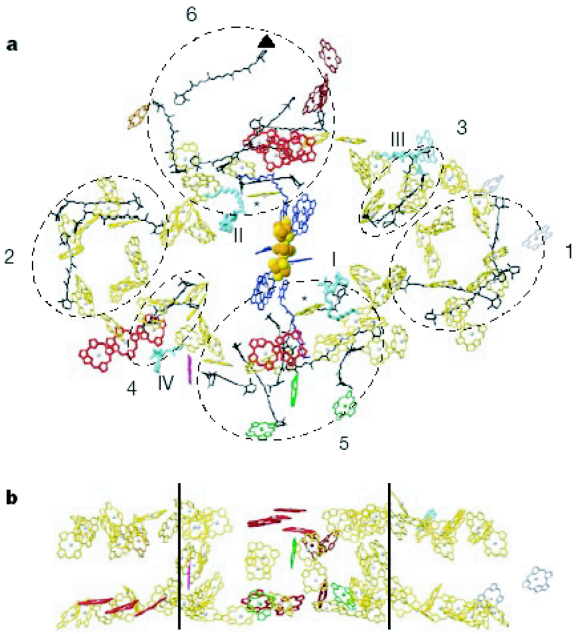

Figure 25. The arrangement of antenna chlorophylls and b-carotenes relative to the electron transfer chain in the PS I reaction center. (a) Top view from the stromal side showing the three iron-sulfur clusters (yellow), the six photoactive chlorophylls (purple), the antenna chlorophylls on PsaA/PsaB (yellow) on peripheral subunits (other colors) and the b-carotenes (black). The latter are clustered in the six regions shown in dotted lines. The four lipids associated with PS I are depicted with Roman numberals. (b) Side view showing the inhomogeneous distribution of chlorophyll molecules near the stromal edge and near the luminal edge of the Photosystem I complex. Reproduceed with permission from Jordan et al., 2001; http://www.nature.com/

3.6.9. Details of Photosystem I: Algae and Higher Plants

Photosystem I in algae and higher plants is accompanied by a light-harvesting complex I which is composed of four different subunits. Each of these subunits is a dimer, consisting of either Lhca1/Lhca4, Lhca2/Lhca2 or Lhca3/Lhca3. Two copies of Lhca1/Lhca4 and one copy each of Lhca2/Lhca2 and Lhca3/Lhca3 are thought to bind to one side of the plant Photosystem I complex as revealed by high-resolution electron microscopy (Figure 26).

PsaM and probably PsaX are missing in algal and plant Photosystem I complexes, but up to new proteins are present, PsaG, PsaH, PsaN and PsaO. It is reasonable to assume that these low molecular mass polypeptides play a role in binding or energy transfer from the light-harvesting complex I proteins. One should note that PsaL is present in plant Photosystem I; the latter exists as a monomer in the memberane, and hence PsaL must have a role in addition to trimerization of the reaction center.

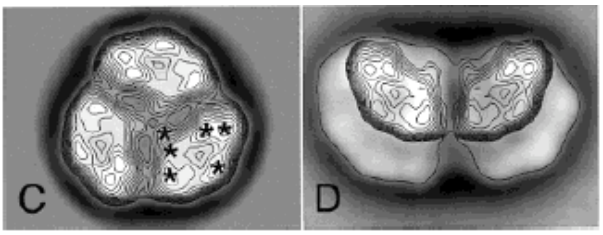

Figure 26. Comparison of the Photosystem I trimer from cyanobacteria (C) with a Photosystem I dimer from higher plants (D). The core region of PS I is superimposed on the higher plant dimer on the right. The remaining density indicates the position of the four LHCI light-harvesting chlorphyll-proteins. Reprinted with permission from Boekema et al., 2001; Copyright (2001), American Chemical Society.

Problem 9. Assuming a solar irradiance of 1000 μEinsteins m^{-2} sec^{-1} calculate how photons are absorbed by a chlorophyll molecule each second. (One Einstein is a mole of photons.) Assume the chlorin ring of a chlorophyll *a* molecule is circular with a radius of 8 Å. If there were fast and efficient energy transfer between individual chlorophyll molecules, how many would need to cooperate to sustain a rate of electron transfer of 300 e^- reaction $center^{-1}$ sec^{-1}? Compare this with the number of chlorophylls in the Photosystem I core and peripheral antenna proteins that serve one P700. Is photosynthesis optimized for high light or low light conditions?

3.7. Unifying Themes in Photosynthesis: a Common Photochemical Motif in all of Nature

In this last section, we will see that all known photosynthetic reaction centers share a common photochemical motif.

3.7.1. Unifying Themes in Photosynthesis: The Reaction Centers in Green Sulfur Bacteria

Just as Photosystem II has a bacterial counterpart in the purple bacterial reaction center, Photosystem I has a bacterial counterpart in green sulfur bacteria (i.e. *Chlorobium tepidum*) and heliobacteria. The reaction centers in these strict anaerobes have not been extensively studied, but they are known to contain a dimeric bacteriochlorophyll *a* (P895) as the special pair, a monomeric chlorophyll *a* as the acceptor, and iron-sulfur clusters as terminal electron acceptors. They are therefore classified as Type I reaction centers.

Nevertheless, there are several differences with Photosystem I. One is that, in spite of considerable effort, quinones have not been proven to participate in forward electron transfer. Another is that the reaction center is a homodimer rather than a heterodimer. Finally, there are fewer polypeptides in these reaction centers. In *Chlorobium tepidum*, the reaction center only consists of 5 polypeptides: a homodimeric core, a bound cytochrome c_{551}, a PsaC-like 2[4Fe-4S] protein, and a low molecular mass protein of unknown function. The antenna structure is also different; in the green sulfur bacteria, about 150,000 to 200,000 chlorophyll molecules self-assemble without protein within a specialized 'sack-like' structure called the chlorosome. This is probably a specialized adaptation to life in a very low light environment.

An unusual, water-soluble antenna protein, termed the Fenna-Matthews-Olson (FMO) protein, is also found between the chlorosome and the reaction center. The crystal structure of this protein was solved decades ago; what makes it special is the absence of carotenoids. It may serve as a conduit for excitation energy from the chlorosome antenna chlorophylls to the reaction center. Little structural information exists on the green sulfur bacterial reaction center apart from some scanning transmission electron micrographs of the latter that show a dimer with two centers of mass on each side of a cavity, as expected for a homodimer.

3.7.2. Unifying Themes in Photosynthesis: Type I and Type II Reaction Centers

It is now clear that all biological reaction centers share a common motif in terms in the early stages of photochemical charge separation. The primary differences between the Type I and Type II reaction centers exist on the electron acceptor side.

In Type II reaction centers, the electron moves from a fixed quinone to a mobile quinone in a two-electron and two-proton charge accumulation process. The released hydroquinol remains within the membrane phase.

In Type I reaction centers, a single electron is vectored out of the membrane phase into the stromal/cytoplasmic phase from a fixed quinone through a series of three iron-sulfur clusters, to soluble ferredoxin. The similarity of the bacterial reaction center with Photosystem II, and the similarity of the green sulfur bacterial and heliobacterial reaction centers with Photosystem I has been evident for a number of years, but the relationship between the Type I and Type II reaction centers as a whole has only recently become evident on both the structural and functional level.

The relationship between the reaction center and antenna polypeptides in Photosystem I, Photosystem II and the purple bacterial reaction center is depicted in Figure 27. The six N-terminal □-helices of Photosystem I are analogous to the six □-helical proteins CP43 and CP47 in Photosystem II. The five C-terminal □-helices of PS I are analogous to

the five α-helices in the D1 and D2 of Photosystem II and to the helices of the L and M subunits of the bacterial reaction center.

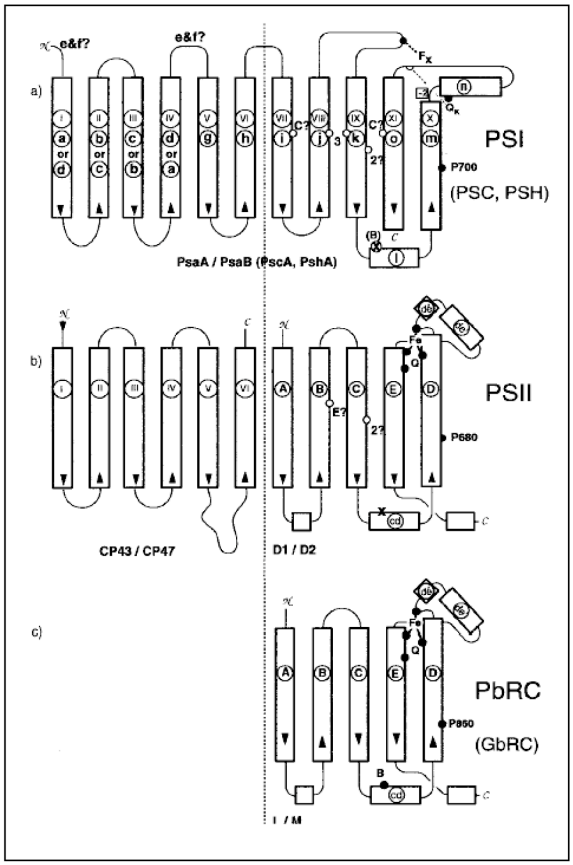

Figure 27. Schematic depiction of the polypeptides that comprise the antenna and reaction center portion of Photosystem I (PS I), Photosystem II (PS II) and the purple bacterial reaction center (PbRC). Note that the antenna chlorophyll proteins comprise the six N-terminal a-helices, and that the reaction center core comprises the five C-terminal a-helices of PsaA and PsaB. Their counterparts in Photosystem II are CP43 and CP47, which represent the antenna chlorophyll proteins, and D1 and D2, which represent the reaction center core proteins. D1 and D2, in turn, are analogous to the L and M polypeptides of the purple bacterial reaction center. The latter contain a separate set of antenna chlorophyll proteins that are unrelated to those in Photosystem I or Photosystem II. J Mol Biol 280, 'A common ancestor for oxygenic and anoxygenic photosynthetic systems: A comparison based on the structural model of photosystem I', Schubert WD, Klukas O, Saenger W, Witt HT, Fromme P, Krauß N., pp. 297-314. Copyright (1998), with permission from Elsevier.

Thus, Photosystem I is a bipartite protein that contains two distinct domains associated with light harvesting and charge-separation. The Photosystem I and Photosystem II polypeptides share only 14% sequence similarity in cyanobacteria. The similarity with the bacterial reaction center is barely over that predicted by chance.

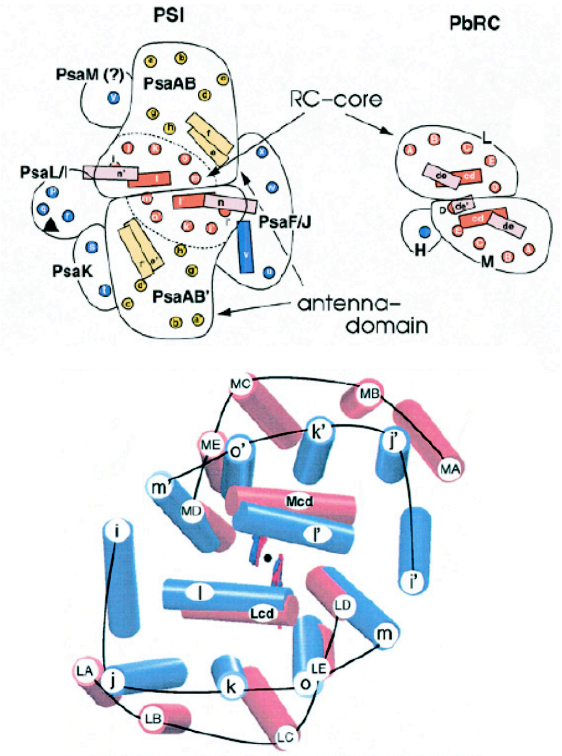

Figure 28. The relationship between the central core region of PS I with the purple bacterial reaction center. (Top) Both reaction centers consist of a heterodimer, each of which is composed of five transmembrane helices and two surface helices. Each subunit of PS I additionally contains six additional a-helices on the C-termini, which binding chlorophyll and serve as to increase the optical cross-section. (Bottom) A superposition of the transmembrane a-helices in the bacterial reaction center (red) and the central transmembrane a-helices in PS I. The primary electron donors are superimposed exactly in this depiction. Reproduced with permission from Schubert et al., 1998. J Mol Biol 280, 'A common ancestor for oxygenic and anoxygenic photosynthetic systems: A comparison based on the structural model of photosystem I', Schubert WD, Klukas O, Saenger W, Witt HT, Fromme P, Krauß N., pp. 297-314. Copyright (1998), with permission from Elsevier

Yet, the three dimensional arrangement of the five C-terminal polypeptides in Photosystem I closely matches the three dimensional arrangement of the D1/D2 polypeptides in Photosystem II. Indeed, they even resemble the three dimensional arrangement of polypeptides in the L/M subunits of the bacterial reaction center (Figure 28).

Similarly, the three dimensional arrangement of polypeptides in the six core antenna helices of Photosystem I closely matches the three-dimensional arrangement of polypeptides in the antenna proteins, CP43 and CP47.

Type II: Quinone Type

Photosystem II	P_{680}	B	I	Q_A	$Fe\ Q_B$
	$(Chl\ a)_{1\ or\ 2}$	*Chl a*	*Ph*	*Plastoquinone*	*Plastoquinone*
Purple Bacteria	$P_{870/960}$	B	I	Q_A	$Fe\ Q_B$
	$(BChl)_2$	*BChl*	*BPh*	*Ubi/Menaquinone*	*Ubiquinone*

Type I: Iron-Sulfur Type

Photosystem I	P_{700}	B	A_0	A_1	$[F_X\ F_A\ F_B]$
	$(Chl\ a)_2$	*Chl a*	*Chl a*	*Phylloquinone*	*3 [4Fe-4S]*
Green Bacteria	P_{840}	?	A_0	?	$[F_X\ F_A\ F_B]$
	$(BChl\ a)_2$		$BChl_{663}$	*Menaquinone?*	*3 [4Fe-4S]*

Figure 29. The relationship between Type II (Photosystem II and the purple bacterial reaction center) and Type I (Photosystem I and the green sulfur bacterial reaction center). A bridging chlorophyll and a quinone have not been identified in the green bacterial reaction center, and there is some indication that the latter may not exist. This would be the first anomaly among an otherwise unified structural and functional motif for the early electron transfer cofactors in photosynthetic systems. Note that the motif breaks down at the terminal electron acceptors; hence, the alternate name 'quinone' type and 'iron-sulfur' type reaction centers for Type II and Type I reaction centers, respectively.

It therefore appears that but one overwhelmingly successful design strategy has evolved in nature to cope with the problem of generating and stabilizing light-induced charge separation so as to produce a high quantum yield (Figure 29). The differences between the reaction centers are one of details; important details to be certain, such as the need to attain different redox potential spans in Photosystem I and Photosystem II so as to reduce $NADP^+$ and oxidize water, respectively (Figure 30).

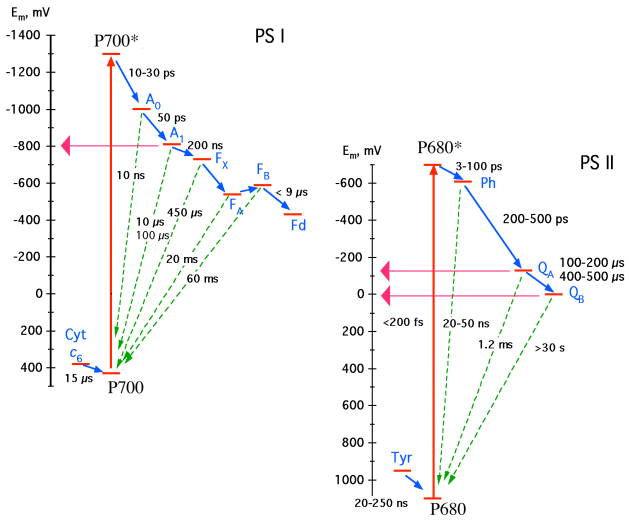

Figure 30 A comparison of the redox potentials of Photosystem I with Photosystem II. Note that the primary electron donors and the quinones are offset from one another by about 700 mV. The cofactors are highly similar in both instances, indicating that the protein environment is what modulates the midpoint potential of a given electron transfer component.

What is fascinating is that the same photochemical motif is capable of poising the primary donor of Photosystem II, P680, at ca.1 V and the primary donor of Photosystem I, P700, at +400 mV, and of poising plastoquinone in the Q_A site of Photosystem II at ca. 0 V and the phylloquinone in the A_1 site of Photosystem I at ca. –800 mV.

The challenge for the future will be to discover how the protein environment modulates the redox potentials of the electron transfer cofactors so that the diverse activities such as $NADP^+$ photoreduction and water splitting can be carried out within the environment of a biological membrane [See Chapter I, section I-10 in this textbook].

Problem 10. The release of one dioxygen molecule requires the transfer of four electrons from two molecules of water to two molecules of $NADP^+$. Given the $E_{m,7}$ of the $2H_2O$ <-> $2H^+ + O_2$ couple as +0.82 V and the $E_{m,7}$ of the $NADP^+ + 2\ e^- + H^+$ <-> NADPH couple as –0.32 V, and given the energies of the photons absorbed by Photosystem II and Photosystem I from Problem 1, calculate the net thermodynamic efficiency of the electron transfer steps in photosynthesis. Note that this is a minimum value, due to additional energy stored in a protonmotive gradient that leads to ATP production.

Acknowledgments

I thank William Cramer and Donald Bryant for a critical reading of this chapter and for many helpful suggestions. This material is based upon work supported by the National Science Foundation under Grant MCB-0117079 and by the Department of Energy under Grant DE-FG02-98ER20314.

References

Antonkine ML, Jordan P, Fromme P, Krauß N, Golbeck J, Stehlik D. 2003. Assembly of protein subunits within the stromal ridge of Photosystem I. Structural changes between unbound and sequentially-bound PS I-bound polypeptides and correlated changes of the magnetic properties of the terminal iron-sulfur clusters. J. Mol. Biol. 327: 671-697.

Antonkine ML, Liu G, Bentrop D, Bryant DA, Bertini I, Luchinat C, Golbeck JH, Stehlik D. 2002. Solution structure of the unbound, oxidized Photosystem I subunit PsaC, containing [4Fe-4S] clusters F_A and F_B: a conformational change occurs upon binding to Photosystem I. J Biol Inorg Chem 7:461-472.

Bittl R, Zech SG. 2001. Pulsed EPR spectroscopy on short-lived intermediates in Photosystem I. Biochim Biophys Acta 1507:194-211.

Boekema EJ, Dekker JP, Van Heel MG, Rögner M, Saenger W, Witt I, Witt HT. 1987. Evidence for a trimeric organization of the photosystem I complex from the thermophilic cyanobacterium *Synechococcus* sp. FEBS Lett. 217:283-286.

Boekema EJ, Dekker JP, Rögner M, Witt I, Witt HT, Van Heel M. 1989. Refined analysis of the trimeric structure of the isolated photosystem I complex from the thermophilic cyanobacterium *Synechococcus* sp. Biochim. Biophys. Acta 974:81-7.

Boekema EJ, Jensen PE, Schlodder E, van Breemen JF, van Roon H, Scheller HV, Dekker JP. 2001. Green plant photosystem I binds light-harvesting complex I on one side of the complex. Biochemistry 40:1029-36.

Boudreaux B, MacMillan F, Teutloff C, Agalarov R, Gu F, Grimaldi S, Bittl R, Brettel K, Redding K. 2001. Mutations in both sides of the Photosystem I reaction center identify the phylloquinone observed by electron paramagnetic resonance spectroscopy. J Biol Chem 276:37299-37306.

Chitnis PR. 2001. Photosystem I: Function and Physiology. Annu Rev Plant Physiol Plant Mol Biol 52:593-626.

Falzone CJ, Kao YH, Zhao JD, Bryant DA, Lecomte JTJ. 1994. Three-dimensional solution structure of PsaE from the cyanobacterium *Synechococcus* sp. strain PCC 7002, a photosystem I protein that shows structural homology with SH3 domains. Biochemistry 33:6052-6062.

Golbeck J. 1992. Structure and function of Photosystem-I. Annual Review of Plant Physiology and Plant Molecular Biology 43:293-324.

Golbeck JH. 1994. Photosystem I in Cyanobacteria. In: Bryant DA, editor. The Molecular Biology of Cyanobacteria. The Netherlands: Kluwer Academic Publishers. p 179-220.

Golbeck JH. 1995. Resolution and Reconstitution of Photosystem I. In:

Song P. S. and Horspeels, W. M., editorw. CRC Handbook of Organic Photochemistry and Photobiology. Bocca Raton, FL: CRC Press. p 1407-1419.

Golbeck JH. 1999. A comparative analysis of the spin state distribution of *in vivo* and *in vitro* mutants of PsaC. A biochemical argument for the sequence of electron transfer in Photosystem I as F_X -> F_A -> F_B -> ferredoxin/flavodoxin. Photosyn. Res. 61:107-149.

Golbeck JH. 2001. Iron-sulfur clusters in Type I reaction centers. Biochim. Biophys. Acta. 1507: 139-160.

Hastings G, Kleinherenbrink FAM, Lin S, Mchugh TJ, Blankenship RE. 1994. Observation of the teduction and teoxidation of the primary electron acceptor in Photosystem I. Biochemistry 33:3193-3200.

Joliot P, Joliot A. 1999. *In vivo* analysis of the electron transfer within Photosystem I: are the two phylloquinones involved? Biochemistry 38:11130-11136.

Jordan P, Fromme P, Witt HT, Klukas O, Saenger W, Krauß N. 2001. Three dimensional structure of Photosystem I at 2.5 Å resolution. Nature 411:909-917.

Krauß N, Hinrichs W, Witt I, Fromme P, Pritzkow W, Dauter Z, Betzel C, Wilson KS, Witt HT, Saenger W. 1993. 3-Dimensional structure of System-I of photosynthesis at 6 Å resolution. Nature 361:326-331.

Krauß N, Schubert WD, Klukas O, Fromme P, Witt HT, Saenger W. 1996. Photosystem I at 4 Å resolution represents the first structural model of a joint photosynthetic reaction centre and core antenna system. Nature Struct Biology 3:965-973.

Moser CC, Keske JM, Warncke K, Farid RS, Dutton PL. 1992. Nature of biological electron transfer. Nature 355:796-802.

Ohnishi T, Sled VD, Yano T, Yagi T, Burbaev DS, Vinogradov AD. 1998. Structure-function studies of iron-sulfur clusters and semiquinones in the NADH-Q oxidoreductase segment of the respiratory chain. *Biochim. Biophys. Acta* 1365:301-308.

Page CC, Moser CC, Chen X, Dutton PL. 1999. Natural engineering principles of electron tunnelling in biological oxidation-reduction. Nature 402:47-52

Schubert WD, Klukas O, Krauß N, Saenger W, Fromme P, Witt HT. 1997. Photosystem I of *Synechococcus elongatus* at 4 Å resolution: comprehensive structure analysis. J Mol Biol 272:741-769.

Schubert WD, Klukas O, Saenger W, Witt HT, Fromme P, Krauß N. 1998. A common ancestor for oxygenic and anoxygenic photosynthetic systems: A comparison based on the structural model of photosystem I. J Mol Biol 280:297-314.

Sétif P, Brettel K. 1993. Forward electron transfer from phylloquinone-A(1) to iron sulfur centers in spinach Photosystem-I. Biochemistry 32:7846-7854.

Sétif P, Bottin H. 1994. Laser flash absorption spectroscopy study of ferredoxin reduction by Photosystem I in *Synechocystis* sp. PCC 6803: Evidence for submicrosecond and microsecond kinetics. Biochemistry 33:8495-8504.

Shen G, Zhao J, Reimer SK, Antonkine ML, Cai Q, Weiland SM, Golbeck JH, Bryant DA. 2002. Assembly of photosystem I. I. Inactivation of the *rubA* gene encoding a membrane-associated rubredoxin in the cyanobacterium *Synechococcus* sp. PCC 7002 causes a loss of photosystem I activity. J Biol Chem 277:20343-20354.

Shen G, Antonkine ML, van der Est A, Vassiliev IR, Brettel K, Bittl R, Zech SG, Zhao J, Stehlik D, Bryant DA, Golbeck JH. 2002. Assembly of photosystem I. II. Rubredoxin is required for the *in vivo* assembly of F_X in *Synechococcus* sp. PCC 7002 as shown by optical and EPR spectroscopy. J Biol Chem 277:20355-20366.

Vassiliev IR, Antonkine ML, Golbeck JH. 2001. Iron-sulfur clusters in type I reaction centers. Biochim Biophys Acta 1507:139-60.

Watanabe T, Kobayashi M, Hongu A, Nakazato M, Hiyama T, Murata N. 1985. Evidence that a chlorophyll a' dimer constitutes the photochemical reaction

center 1 (P700) in photosynthetic apparatus. FEBS Lett. 191:252-256.
Witt I, Witt HT, Gerken S, Saenger W, Dekker JP, Roegner M. 1987. Crystallization of reaction center I of photosynthesis. Low-concentration crystallization of photoactive protein complexes from the cyanobacterium *Synechococcus* sp. FEBS Lett. 221:260-264.
Xia Z, Broadhurst RW, Laue ED, Bryant DA, Golbeck JH, Bendall DS. 1998. Structure and properties in solution of PsaD, an extrinsic polypeptide of Photosystem I. Eur J Biochem 255:309-316.
Yang F, Shen G, Schluchter WM, Zybailov B, Ganago AO, Vassiliev IR, Bryant DA, Golbeck JH. 1998. Deletion of the PsaF polypeptide modifies the environment of the redox-active phylloquinone. Evidence for unidirectionality of electron transfer in Photosytem I. J. Phys. Chem. 102:8288-8299.
Zhao J, Li N, Warren P, Golbeck J, Bryant D. 1992. Site-directed conversion of a cysteine to aspartate leads to the assembly of a [3Fe-4S] cluster in PsaC of Photosystem- I - The photoreduction of F_A is independent of F_B. Biochemistry 31:5093-5099.
Zouni A, Witt HT, Kern J, Fromme P, Krauß N, Saenger W, Orth P. 2001. Crystal structure of Photosystem II from *Synechococcus elongatus* at 3.8 A resolution. Nature 409:739-743.